Deanship of Graduate Studies
Al-Quds University

SURFACE ROUGHNESS ANALYSIS OF SILVER NANOPARTICLES USING ATOMIC FORCE MICROSCOPY

Ranim Mansour Abd Al Qader Mohamad

M.Sc. Thesis

Jerusalem – Palestine

1446/2025

SURFACE ROUGHNESS ANALYSIS OF SILVER NANOPARTICLES USING ATOMIC FORCE MICROSCOPY

Prepared By:

Ranim Mansour Abd Al Qader Mohamad

B.Sc.: Bethlehem University, Palestine

Supervisor: Dr. Husain Alsamamra

Co-Supervisor: Dr. Ishaq Musa

A Thesis Submitted in Partial fulfillment of requirements for the degree of Master of Science from the Department of Physics, Faculty of Science and Technology, Al-Quds University.

Jerusalem-Palestine

1446/2025

Al-Quds University

Deanship of Graduate Studies

Physics Department

Thesis Approval

SURFACE ROUGHNESS ANALYSIS OF SILVER NANOPARTICLES USING ATOMIC FORCE MICROSCOPY

Prepared By: Ranim Mansour Abd Al Qader Mohamad

Registration No: 22212428

Supervisors:

Dr. Husain Alsamamra

Dr. Ishaq Musa.

Master thesis submitted and accepted, Date: 24-5-2025

The names and signatures of the examining committee members are as follows:

1- Head of Committee: Dr. Husain Alsamamra Signature:

2- Co-Supervisor: Dr. Ishaq Musa Signature:

3- Internal Examiner: Dr. Musa Abuteir Signature:

4- External Examiner: Dr. Jamal Ghaboun Signature:

Jerusalem – Palestine
1446/2025

Dedication

To my beloved and great mother, Hanan, the source of my strength and prayers, the one because of whom this journey began, and for whose eyes this dream was carried to life.

To my supportive father, Mansour, whose quiet encouragement never ceased

To my brothers, Ahmad, Mohamad, and Mu'taz, whose presence is a pillar in my life

To my dear sisters, Majd and Deema, the gentle souls who always cradle me with love and spoil me with tenderness.

To my friends and soul-sisters, Donia and Bayan, for their endless support, laughter, and belief in me.

To my loving husband, Khalid, and our coming daughter, my future, my light.

After God’s grace, what once felt impossible became real, not without their hearts, and never without their hands.

Ranim Mansour Abd Al Qader Mohamad

Declaration

I certify that this thesis submitted for the degree of master is the result of my research, except where otherwise acknowledged, and that this thesis, neither in whole nor in part, has been previously submitted for any degree to any other university or institution.

Signed:

Ranim Mansour Abd Al Qader Mohamad

Date: 24/5/2025

Acknowledgments

Praise be to **Allah**, who granted me strength, success, and ease. who supported me and made the path smooth throughout this journey. To Him belongs all credit, before it began, and after it was done.

I extend my sincere thanks and deep gratitude to my supervisor, **Dr. Husain Alsamamra**, for his support and follow-up throughout the preparation of this Thesis, as well as his guidance and careful monitoring of the research process. I also extend my special thanks to **Dr. Ishaq Musa**, who generously provided me with the necessary academic assistance and data.

In this regard, I cannot stop my deepest gratitude and appreciation to my dear **Family**, **Husband**, and **Friends**, one by one, who have been my true support throughout this journey. Each of them deserves my deepest gratitude for all the types of support they have provided me, they being the best hands ever who gave me unlimited encouragement, which had the greatest impact and the main reason for completing this work.

Ranim Mansour Abd Al Qader Mohamad

Abstract

Since its discovery, nanoscience has revolutionized science. NMs have increasing interest in various scientific and industrial fields, such as electronics, medicine, and the environment, due to their unique properties, which are radically different from bulk materials. Among these properties, surface roughness is one of the most important factors affecting the performance of nanoparticles (NPs), as it plays a crucial role in various types of chemical reactions and surface properties. Therefore, understanding and studying this property is essential to developing NPs applications.

In this context, the surface roughness of nanoparticles is affected by several factors, which may occur during or after the synthesis process, or during the scanning process. The most prominent of these factors are the size of the NPs, their concentration during the synthesis process, the type of tip used for measurement, and the synthesizing method used, which is a fundamental and powerful differentiating factor.

This study aims to find the relationship between these factors and the surface roughness values measured using an AFM, by comparing between the surface roughness of samples of AgNPs prepared using different methods of synthesis and concentrations, to provide a deep understanding of the factors that control the surface roughness of nanoparticles.

Table of Contents

List of Tables

List of Figures

List of Figures…. Continued

List of Abbreviations

AC	Alternating current
AFM	Atomic Force Micoscopy
Ag	Silver
Ag^{+}	Silver ion
Ag^{0}	Silver atom
$AgNO_3$	Silver Nitrate
AgNPs	Silver Nanoparticles
Al	Aluminum
Ar	Argon
AuNPs	Gold Nanoparticles
Co	Cobalt
Cu	Copper
DC	Direct current
F	Iron
Fig.	Figure
Ga	Gallium
MNPs	Metal Nanomaterials
N	Nitrogen
Ni	Nickel
Nms	Nanomaterials
NP-10	Nanoparticles with 10 mg/50 mL concentration
NP-30	Nanoparticles with 30 mg/50 mL concentration
NP-50	Nanoparticles with 50 mg/50 mL concentration
NP-70	Nanoparticles with 70 mg/50 mL concentration
NPs	Nanoparticles
O	Oxygen
Pt	Platinum
QCM	Quartz crystal monitor

List of Abbreviations…. Continued

QMF	Quadrupole mass filter
Ra	Roughness average
ROS	Reactive Oxygen Species
Rp	Maximum profile peak
Rq	Root mean square roughness
Rv	Maximum profile valley
Rz	Maximum height
S	Silicon
sccm	Standard cubic centimeters per minute
SCNMS	Semiconductor Nanomaterials
SEM	Scanning Electron microscopy
Sn	Stannum
SPM	Scanning probe microscopy
SPR	Surface Plasmon resonance
STM	Scanning tunneling microscopy
TEM	Tunnling Electron Microscopy
UHV	Ultra-high vacuum
Zn	Zinc

Chapter One

Introduction

The first chapter introduces the basic concepts needed to better understand the field of nanotechnology and its applications, which helps in a clearer perception of the nature of the research. Moreover, background information on silver nanoparticles (AgNPs) is given, along with a brief overview of the importance of surface roughness analysis. Finally, the chapter gives a scope of the thesis by clarifying the objectives, the significance of this study, and the research statement.

1.1 Overview

Nanoscience is one of the emerging sciences that is concerned with studying materials and phenomena in very small dimensions, specifically on the nanometer scale, and manipulating them to produce materials with new and amazing characteristics, where properties differ significantly from those found in bulk materials in the macroscopic world (Yousaf & Ali, 2007). Speaking of the prefix “nano” specifically, the word is taken from the Greek word "nanos" (or Latin "Nanos") meaning "dwarf", it has been used in the metric system since 1960 which refers to a factor of 10^{-9}, so a nanometer is one billionth of a meter (Beumer, 2012).

The beginning inspiration for nanoscience came from the famous lecture given by Richard Feynman in 1959 during a conference of the American Physical Society, when he said, “There is plenty of room at the bottom” (Nouailhat, 2006) but it appeared to the public after the invention of the scanning tunneling microscope, which opened the way to photographing and manipulating atoms, which had huge impact on surface science. The field did not stop here, as it was expanded with the invention of the atomic force microscope (AFM), which enabled direct measurement and manipulation of materials on the atomic scale in new ways and possibilities (Lindsay, 2010).

Nanoparticles (NPs) can be defined as particles with a diameter less than 100 nanometers in at least one dimension (Altammar, 2023). They include a wide range of materials like Metal, Carbon, Semiconductor, Ceramic NPs, and more (Khan et al., 2019). These particles consistently exhibit various properties that differ from those of bulk materials, such as changes in the color of NPs, a

decrease in melting temperature, alterations in their magnetic properties, and enhanced catalytic activity, among others.

The reason for this is that these properties depend directly on the size then because the surface area of these particles becomes enormous compared to their small size, different quantum phenomena appear, which explain these new features (Itakovi, 2019). This was not a bad thing; on the contrary, scientists were able to harness these phenomena to open new horizons by applying them in a way that serves all fields and sectors, such as the environment, medicine, pharmaceuticals, agriculture, industries, and many others (V. Singh et al., 2021).

The synthesis of NPs is primarily achieved using various methods, which can be divided into two approaches: The Top-Down approach and the Bottom-Up approach. First, the top-down approach involves breaking bulk materials into smaller structures, resulting in irregularly shaped, extremely small particles through multiple techniques, including chemical, physical, or mechanical methods such as grinding, lithography, milling, and laser processing. Secondly, the bottom-up approach focuses on assembling atoms and clusters together one by one to form NPs in their final form, where the atoms are the building blocks of the required nanostructures. Some of the techniques used in this approach are: Sol-Gel method, Hydrothermal, Chemical vapor deposition, etc (Tripathy, 2023).

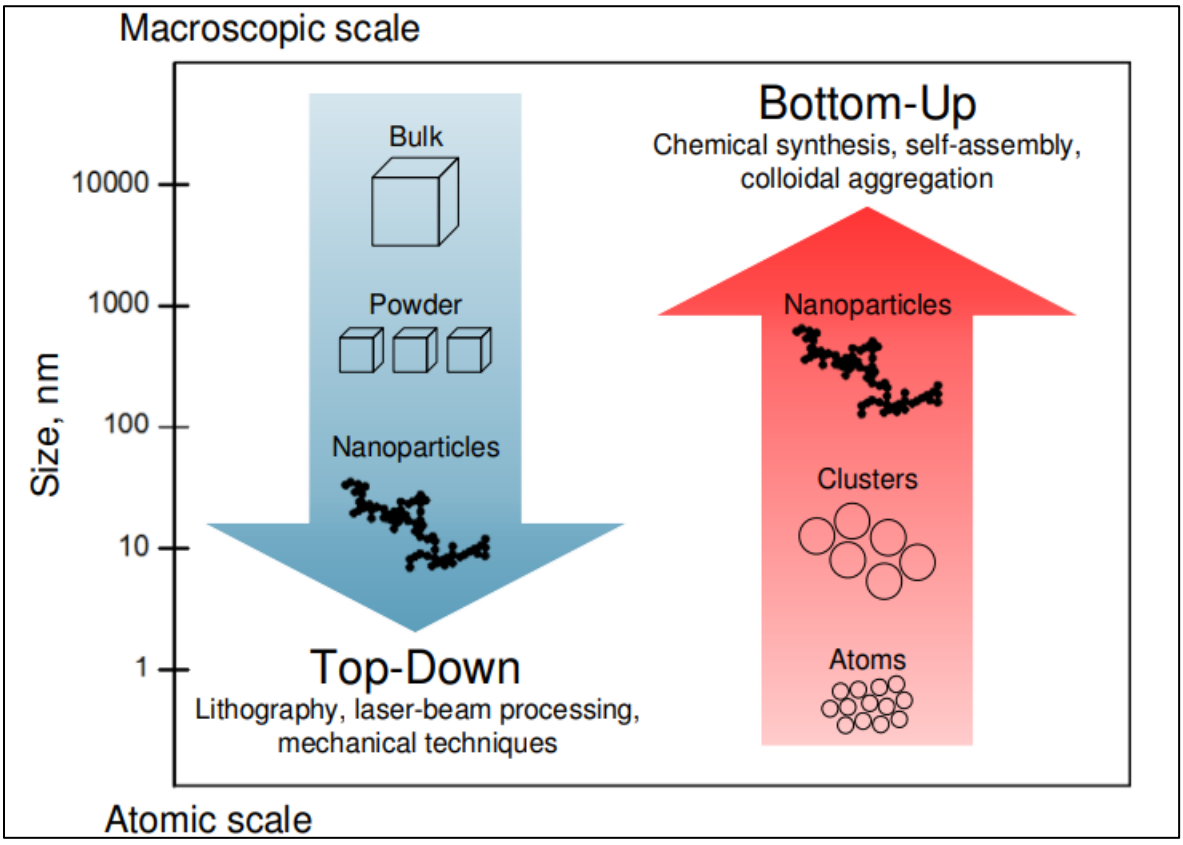

Fig. (3.1): Two approaches of NPs production: top-down and bottom-up (Dutka, 2014).

1.2 Silver Nanoparticles

Certain NPs have been used more than others in research and practical applications based on several criteria. One of the most important and highly demanded NPs is AgNPs. These AgNPs have gained this worth due to their exceptional chemical, physical, and biological properties, such as electrical, optical, and magnetic properties, and their strong antibacterial activity (T. Galatage et al., 2021). Furthermore, they are easy to manufacture and cost-effective compared to other NPs, such as gold nanoparticles (AuNPs) (Beyene et al., 2017).

AgNPs can be formed into a variety of shapes, depending on the manufacturing method and application aim. They can be shaped as spheres, triangles, cubes, rods, and more (Fig. 1.2). For example, allowing for sufficient drug supply, AgNPs as a drug delivery system are made larger than 100 nm. This change in shape and size is closely related to all properties, so it is necessary to study this effect in detail to design the particles in a way suitable for their function (Abbas et al., 2024).

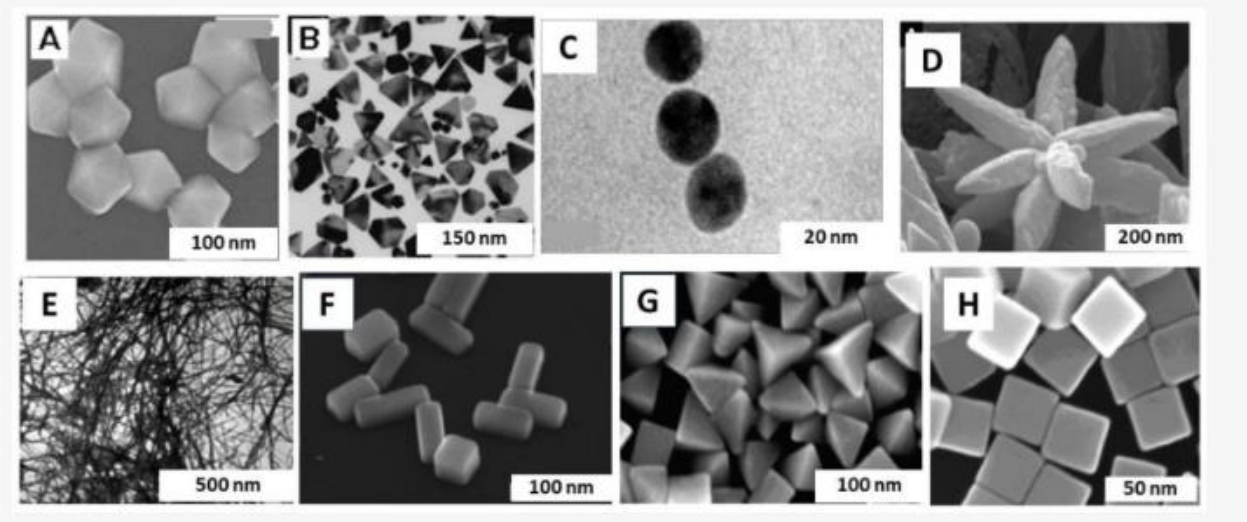

Fig. (1.4): TEM and SEM images for different shapes of AgNPs, (A) Decahedrons, (B) Prisms, (C) Sphere, (D) Flower, (E) Nanowires, (F) Nano-bars, (G) Pyramids, (H) Nano-cubes (Abbas et al., 2024).

1.2.1 Properties and Applications of AgNPs

The properties of AgNPs are largely influenced by their size and shape because of their high surface area-to-volume ratio. Therefore, their properties are different from their bulk size (Zhang et al., 2016). Due to their diverse applications, understanding these properties is critically important.

1) Optical Properties:
   AgNPs exhibit unique and extraordinary optical properties, notably their high absorption and scattering capabilities (Oldenburg, n.d.). When these particles are exposed to light at specific wavelengths, the free electrons on their surfaces are excited, resulting in a coherent collective oscillation of these electrons along the electric field of light. The amplitude of

this oscillation reaches its maximum at a specific frequency known as surface plasmon resonance (SPR) (Ider et al., 2017).

The optical properties of AgNPs, such as absorption and scattering, can be controlled by modifying the particle's shape, size, and surface local refractive index (Mekuye, 2024). For example, larger NPs exhibit higher scattering capacity, with peaks that broaden and longer wavelengths compared to smaller NPs, whose response is mostly light absorption, with shorter plasmon resonance peaks near 400 nanometers (Abbas et al., 2024).

These unique optical properties of AgNPs have numerous applications in industrial, medical, and practical fields. AgNPs play a vital role in developing biosensors and chemical detection due to their high sensitivity and sharp color changes upon binding to target molecules (Mahmudin et al., 2015). They are used in biomedical imaging (Y. Li et al., 2023), the localized thermal ablation of cancer cells (Jouyban & Rahimpour, 2020), also in the designing of coatings and smart optical filters, the detection of pollutants, drugs, and viruses, and the manufacturing of solar cells (Beyene et al., 2017)

2) Electrical Conductivity:

One of the most important properties of bulk silver material is that it has the highest electrical conductivity at room temperature compared to other metals. This is due to their atomic structure and a single valence electron in their outer shell, which is not tightly bound to the nucleus (Kockert et al., 2019). This allows for the flow of electric current with minimal resistance when an electric field is applied (Varga et al., 2012).

Despite changing material properties at the nanoscale, the AgNPs retain their exceptional electrical conductivity and show enhanced surface interactions (Duman et al., 2024). This is due to the large surface-to-volume ratio of the AgNPs, which increases the contact points between the particles, enabling more efficient charge transfer (Fang & Lafdi, 2021).

This property has been widely utilized in a variety of applications. It has recently been used in developing temperature and pressure sensors due to its excellent electrical response, opening the way for manufacturing fast and low-cost sensors that can be integrated into modern robots and medical devices (Duman et al., 2024). It is also widely used in the printed electronics industry, producing electronic inks that can be directly printed on fabric, paper, and plastic (Chen et al., 2009). Moreover, it is used in manufacturing wireless devices and antennas, especially small ones such as phones, which are distinguished by their high efficiency (Alshehri et al., 2012).

3) Antimicrobial Activity:

Using silver as an antimicrobial did not begin with the discovery of nanoscience. It has been widely used in this field for nearly 5,000 years due to its unique antimicrobial properties and non-toxicity to humans (Panja, 2021). With the advancement of nanotechnology, it has been proven that AgNPs retain these properties even better due to their high surface-to-volume ratio and ability to control the particles' size, shape, surface area, and surface charge (Duman et al., 2024).

In bacterial cells, for example, AgNPs have a tremendous ability to disrupt and even rupture the cell membrane (Menichetti et al., 2023). They can also disrupt protein synthesis by either generating reactive oxygen species (ROS) or interacting with thiol groups in vital bacterial proteins and enzymes (H. Li et al., 2016). This results in complexes that weaken the cell or often lead to its death, without affecting the surrounding healthy cells (Marambio-Jones & Hoek, 2010). This has been applied in several fields, such as food

packaging and the production of materials used in dentistry, to reduce the risk of bacterial disease (Bapat et al., 2018).

Sometimes, using the same antibacterial mechanism, but sometimes using different mechanisms, AgNPs also have significant antifungal (Żarowska et al., 2019), antiviral (Naumenko et al., 2023), anti-inflammatory (T. Galatage et al., 2021), and anticancer properties that limit tumor growth and spread (Abass Sofi et al., 2022). Regardless of the mechanism, the activity of AgNPs depends on their surface modification. For example, smaller AgNPs are more effective as antivirals than larger ones due to their larger surface areas (Elechiguerra et al., 2005). These properties have been applied in breakthrough fields such as wound dressings, bone repair, medical surface coatings, cosmetics, textiles, drug carriers, imaging, water treatment, and more (Panja, 2021).

1.2.2 Synthesis of AgNPs

AgNPs are synthesized using two approaches, as mentioned above: top-down or bottom-up. The methods used in each approach are classified as chemical, physical, and biological (green synthesis) (Yaqoob et al., 2020). Each method has advantages and disadvantages, but they all agree that different synthesis methods lead to various properties, characteristics, and shapes of the resulting AgNPs. Therefore, the synthesis method is chosen based on available capabilities and the intended function of the AgNPs.

1. Chemical Methods:

   Chemical synthesis of AgNPs is one of the most popular methods to date, despite the danger of the chemicals used and the waste generated by the process, which are harmful to humans and the environment (Sportelli et al., 2018). This is explained by its ease of use, low cost compared to other methods, and ease of producing large numbers of AgNPs (Nie et al., 2023).

   Several techniques have been developed in this field, such as chemical reduction and microemulsion techniques (Z. Li et al., 2020). Chemical reduction is the most popular of these methods, requiring three factors (Iravani et al., 2014): a silver salt starting material such as silver nitrate, a chemical reducing agent such as citrate (Khatoon et al., 2017), and stabilizing and capping agents such as polymers (Fahim et al., 2024). The role of reducing agents is to reduce the silver ion (Ag^{+}), derived from the salt, by adding an electron, converting it into AgNPs (Ag^{0}). After that, the stabilizing and capping agents control the particles' size and prevent them from agglomerating after synthesis (Lee & Jun, 2019).
2. Physical Methods:

   Physical synthesis methods harness various forms of energy to produce AgNPs. For example, mechanical energy is used, as in ball milling, which involves placing metallic components in a rotating container filled with an inert gas and containing grinding balls of specific masses. The materials are ground by the high-pressure motion of the balls, resulting in NPs whose properties are affected by the duration of grinding and the factors used (Khayati & Janghorban, 2012). These particles are susceptible to agglomeration due to the lack of a coating agent(Lee & Jun, 2019). Thermal energy can also be used, as in the evaporation–condensation approach (Stagon & Huang, 2013); electrical energy, as in the electric arc discharge method (Tien et al., 2008); and optical energy, as in the laser ablation method (Amendola & Meneghetti, 2009).

These methods produce clean, highly purified particles due to the absence of chemical materials such as reducing agents and stabilizers. This means the absence of toxic substances that threaten human health and the environment. As laser ablation method is considered a pure and non-polluting method (Güzel & Erdal, 2018). However, there are certainly disadvantages, including high costs primarily due to the need for advanced equipment, high energy consumption, slower synthesis times, so it needs a longer time, and lower yield potential. The evaporation and condensation approach requires a tube furnace, which combines all these disadvantages and also requires large storage space (Nguyen et al., 2023).

3. Green synthesis:

In alignment with global sustainable development goals, scientists have developed a new, clean alternative method for synthesizing AgNPs. This method uses living organisms such as microbes, plants, fungi, and others to synthesize metallic NPs, which provide environmentally friendly, non-toxic reducing and coating agents and are considered a potential alternative to chemical methods (Liaqat et al., 2022).

Green synthesis offers an alternative that treats the disadvantages of physical and chemical methods. It has proven to be cost-effective, easy to use, with higher yields, faster synthesis times, and environmental safety (Veerasamy et al., 2011). The different media used to produce the particles result in significantly different properties. Therefore, the shapes, diameters, and surface specifications of bio-produced AgNPs vary, affecting their performance. This presents a challenge for researchers to develop a method that enables them to control the properties of the resulting particles to suit their function (Habeeb Rahuman et al., 2022).

Plants have been used in green synthesis by extracting various parts, such as bark, roots, stems, flowers, fruits, seeds, leaves, and peels, and using them as incubators for particle synthesis. The enzymes act as reducing agents, and the proteins act as stabilizing agents. Some plants that have proven effective for producing AgNPs include turmeric, pomegranate, aloe vera, banana peels, thyme, ginger, basil, garlic, and others (Siddiqi et al., 2018).

As for living microorganisms, bacteria, such as Bacillus licheniformis, have been extensively used in this field, with their internal cellular components acting as reducing and stabilizing agents. Yeast, a fungus, and the algae Pyrulina, a microalga, have also been successful in synthesizing AgNPs. All three produced particles with various shapes and properties, including spheres, triangles, cubes, and hexagons (Nguyen et al., 2023). However, plant-based synthesis is significantly faster in terms of productivity (Mustapha et al., 2022).

Table 1.1: A comparison between the 3 methods for synthesizing AgNPs (Chemical, Physical, Green).

	Chemical synthesis	Physical synthesis	Green synthesis
Advantages	*Control of particle size and shape *High productivity *Low cost *Easy	*High purity *No harmful chemicals used	*Non-toxic to humans *Environmentally friendly *Easy *Low cost
Disadvantages	*Use of toxic chemicals *Harmful to the environment	*Advanced equipment needed *High cost	Difficulty controlling the resulting particles
Common Applications	Industrial and research applications such as electronics	Sensitive applications requiring high-purity materials	Medical and pharmaceutical applications as Biosensing

1.3 Surface Roughness Analysis

One of the most important properties when studying NPs is surface roughness, which describes the surface texture and indicates the degree of deviation from a perfect smooth surface. Manufacturing processes and other factors produce bumps and irregularities on surfaces, which determine how particles interact with their surroundings and determine their physical and chemical properties, especially in NPs due to their large surface area compared to their particle size (Myshkin & Grigoriev, 2013).

Studies have shown that studying the surface roughness of NPs helps improve the properties required for various scientific, medical, and industrial fields. The importance of studying surface roughness can be summarized in several key points that expand into more sub-applications (Gulumian et al., 2021). First, understanding surface roughness and the factors affecting it helps increase the effective surface area at the nanoparticle, as in chemical catalysis applications, where it has been proven that increasing surface roughness increases the number of active sites, which increases reaction efficiency and improves catalytic activity (Jiang et al., 2020). Second, improving adhesion. A common application in this field is coatings, as increasing the surface roughness of NPs increases the bonding and entanglement forces between different media, resulting in better results (Ravi et al., 2017). Third, improving the stability of NPs, meaning their resistance to unwanted agglomeration and deposition by increasing surface roughness, as in

solutions (Olarte-Plata et al., 2020). Fourth, improving particle solubility, as in pharmaceutical and environmental applications, where experiments have proven that increasing surface roughness is an effective strategy for improving nanoparticle solubility in various solvents (Vaculikova et al., 2016). Fifth: More efficient drug delivery. Research has been conducted on NPs with rough surfaces to discover their role in drug delivery. The results indicate the success of the process, proving that the surface roughness of NPs affects their performance in drug release (Xue et al., 2022; Abdelkawi et al., 2023). Sixth: Improving optical properties. The interaction of NPs with light is affected by their surface roughness. Modifying surface roughness contributes to modifying the particle's response to optical phenomena such as SPR. One of the most important applications is photovoltaic cells, as studies have proven that increased surface roughness increases light-trapping efficiency in cells (Alkhalayfeh et al., 2022). Seventh: Increasing the sensitivity of sensors. Studies have shown that the performance of various types of sensors can be improved by increasing the surface roughness of NPs, resulting in more active sites and, consequently, increased sensitivity (Treebupachatsakul et al., 2021).

1.4 Objectives

This study encompasses an analysis of the surface roughness of AgNPs, evaluated through various parameters and methodologies, as outlined below:

1. Variation in surface roughness correlated with NPs size.
2. Dependency of surface roughness on the concentration of NPs during synthesis.
3. Comparison of surface roughness measurements using different AFM tips: standard and sharp.
4. Influence of synthesis techniques on surface roughness, comparing physical and green methods.

Chapter Two

Literature Review

Chapter Two reviews the literature related to this study's basic concepts, aiming to provide a comprehensive overview that helps interpret the research stages and analyze and discuss the results. This chapter reviews nanomaterials (NMs) and their classifications, including semiconductor and metallic NMs. It also highlights the most prominent methods used to analyze the surface roughness of AgNPs, explaining the factors affecting roughness measurements to facilitate the interpretation and comparison of results.

2.1 Nanomaterials

According to a study by Roco (2003), the use of nanotechnology to understand and modify the behavior of atoms and molecules on scales ranging from approximately 1 to 100 nanometers has contributed to the creation of molecular structures and systems that build materials with unique properties, these modified materials are called NMs.

NMs are defined as "a group of materials with at least one of their three dimensions less than 100 nanometers." They are the cornerstone of modern nanotechnology (Alagarasi, 2011). The study explained why these materials have gained additional importance due to their unique electrical, magnetic, optical, physical, and biological properties that differ from those of conventional materials at larger dimensions. These exceptional properties are attributed to the high surface area-to-volume ratio of NMs, which leads to higher chemical activity. In a study by Mekuye & Abera (2023), they fully agreed with this definition, adding that the shape, size, and surface area of NPs play a crucial role in determining their properties, considering them distinct from the four known physical states.

To further understand the small size of NMs, this comparison (Fig.2.1) illustrates how organisms and biological structures vary in size from micro to nano. While red blood cells, human hair, and alveoli are visible at the micrometer scale, viruses and DNA only begin to appear at the nanometer scale.

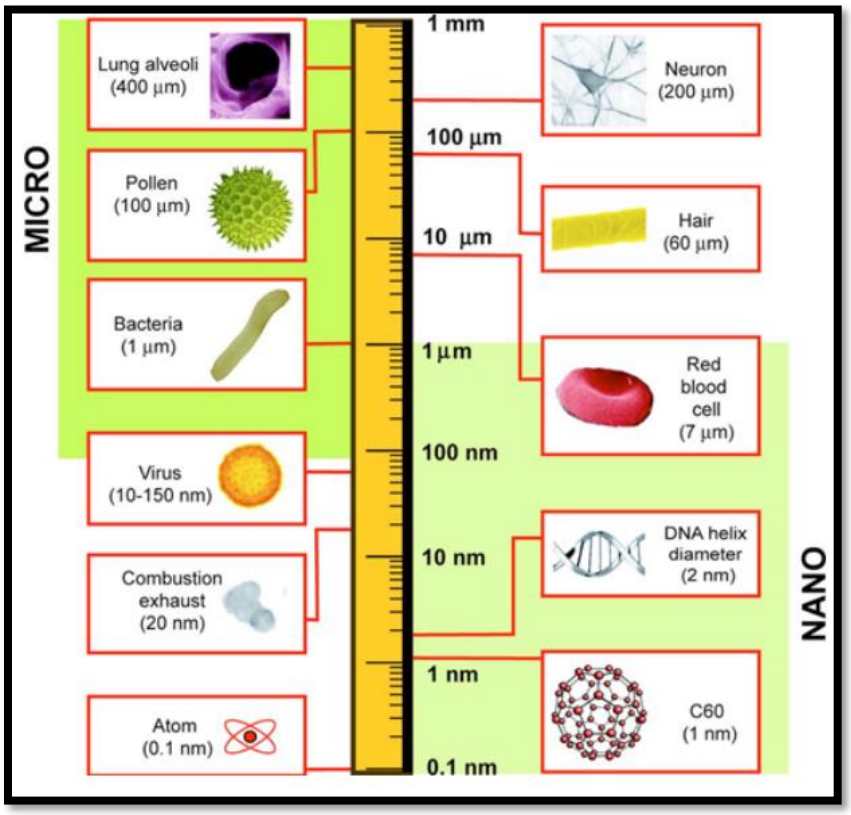

Fig. (2.1): A comparison illustrates the differences between micro and nanoscale dimensions (Buzea et al., 2007)

NMs have been classified based on various criteria, starting with their origin. In the same study conducted by Mekuye & Abera (2023), NMs were classified into natural and artificial. Natural NMs exist in various forms, such as viruses, protein molecules, DNA, minerals, and others. Artificial NMs are consciously and precisely engineered and synthesized according to specific rules and various methods, following either a top-down or bottom-up approach, such as the synthesis of AgNPs.

In terms of dimensions, NMs are classified into four categories according to the Siegel classification (Siegel, 1992), based on the number of dimensions within the nanoscale (1–100 nm) of the three spatial dimensions (x, y, and z). This classification has been adopted in most research related to NMs, as in the study of Alagarasi (2011), Mohapatra (2020), and Mekuye & Abera (2023). The classification is:

1. Zero-dimensional (0D) NMs:
   In this category, all three dimensions are within the nanoscale, such as nanospheres and atomic clusters, giving them unique electronic properties.

2. One-dimensional (1D) NMs:
   Having two dimensions (e.g., x and y) within the nanoscale, while the third dimension is larger than 100 nm. They resemble needle-shaped structures, which include nanowires, nanotubes, rods, and nanofibers.
3. Two-dimensional (2D) NMs:
   Having only one dimension (e.g., x) within the nanoscale, while the other two dimensions extend to larger scales. They take the form of sheets, such as nanofilms and two-dimensional networks.
4. Three-dimensional (3D) NMs:
   None of their dimensions fall within the nanoscale, but they can consist of nanoscale units (0D, 1D, or 2D) interconnected in a volumetric structure. This category includes bulk NMs characterized by the presence of interfaces between different components.

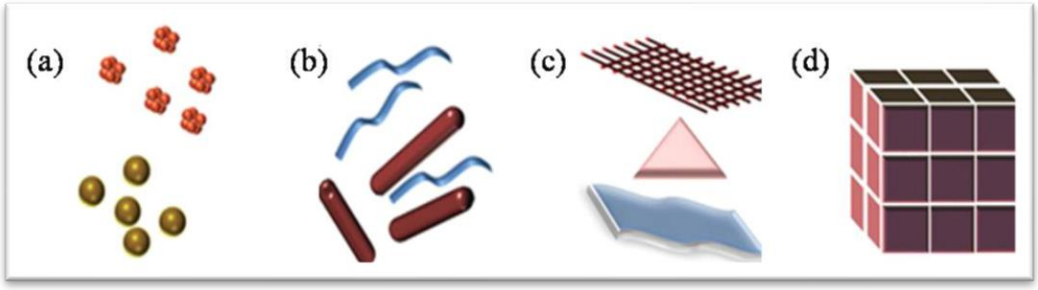

Fig. (2.2): Classification of NMs (a) 0D; (b) 1D; (c) 2D; (d) 3D NMs.

However, in terms of morphological properties, which primarily depend on the aspect ratio to determine the overall shape of the particles, NMs are divided into two main categories: high-aspect-ratio materials and low-aspect-ratio materials. The former includes rectangular or elongated shapes, such as nanotubes, nanorods, and nanowires. Low-aspect-ratio NMs include cubic, spherical, oval, prismatic, and columnar shapes, and these particles may appear as aggregates in the form of powders, colloids, or suspensions. This classification is used to accurately define nanostructure because of its significant impact on the physical and chemical properties and behavior of NMs in various applications (Buzea et al., 2007).

2.2 Semiconductor NMs

After reviewing the general classifications of NMs, it is important to address some important functional categories widely used in technical and scientific applications, including semiconductor NMs (SCNMs). This category is characterized by distinctive electronic and physical properties that make it suitable for a wide range of fields.

According to two studies by Nayak et al. (2017) and Khan et al.(2017), published at different times, semiconductors are described as materials with characteristic features intermediate between metals and nonmetals, and are usually classified according to their constituent elements in the periodic table: groups II–VI as ZnO, III–V as GaN, and IV–VI as SnS. These two references focused on the electronic structure of SCNMs, particularly the possibility of modifying the energy bandgap, whereby the particle size and chemical composition can be tuned to suit the wavelengths appropriate for requested applications, such as in photosensors, solar cells, and imaging devices.

On the other hand, research published by Lo (2024) discussed the structural and surface properties of SCNMs, highlighting their photoelectric and electrochemical performance, focusing on improving their optical response. These SCNMs possess electrical and optical conductivity properties that can be tuned according to the desired function. They are also highly sensitive to environmental conditions such as heat or light, making them suitable for precise applications such as chemical sensors, nanoimaging, and nanoelectronic circuits.

Furthermore, a study by Sahu (2019) highlighted the impact of the manufacturing method of SCNMs on their effectiveness, size, and properties. It demonstrated that they are characterized by broad flexibility depending on their function, due to the diversity of their chemical structures, unlike metallic NMs, which are primarily characterized by their surface and catalytic properties. This is partially consistent with a study by Sayab (2024) for the University of Karbala focusing on using computational methodologies for the theoretical analysis of electronic properties. The result supported experimental hypotheses about the possibility of controlling SCNMs' properties by controlling manufacturing techniques.

Although each study approached SCNMs from a different perspective, they all clearly agreed that the energy gap and electron distribution are the two crucial factors in determining the function of SCNMs.

2.3 Metallic Nanoparticles

Metallic nanoparticles (MNPs) are among the materials that have received significant attention in scientific research despite their small size, due to their unique physical and chemical properties that distinguish them from conventional large-sized materials. They consist of a single element, such as silver (Ag), gold (Au), copper (Cu), and others. This uniqueness has opened up numerous applications for them in various fields, such as technology, medicine, and the environment.

MNPs can be defined as a substance composed of pure metals in the form of individual atoms or clusters of atoms, with dimensions ranging from 1 to 100 nanometers. According to Saleh's study (2022), the most commonly used and applied metallic particles are silver (Ag), gold (Au), platinum (Pt), iron (Fe), copper (Cu), zinc (Zn), cobalt (Co), nickel (Ni), and aluminum (Al). The large surface area relative to their small size, combined with their diverse shapes, sizes, and compositions, gives MNPs a significant advantage over other types of NPs. One of their most remarkable properties is plasmonic resonance (SPR), along with their broad-spectrum light absorption and high chemical reactivity (Chakraborty & Pradeep, 2017). Shahalaei et al. (2024) added that MNPs possess remarkable chemical and biological properties, such as oxidation resistance, effective catalytic properties, and antimicrobial resistance.

Gold and silver NPs are among the most studied and used NPs, but AgNPs have gained greater preference due to their lower cost compared to gold NPs, high antimicrobial activity and anti-infection properties, wound healing processes, and their high effectiveness in medical applications such as disinfectants, bandages, and coatings for surgical instruments. ApNPs have also been successful in targeted drug tests, where they interact effectively with cancer cells and reduce tumor size (Burlec et al., 2023; Jangid et al., 2024).

Conversely, Shahalaei et al. (2024) warned of the possibility of cytotoxicity when AgNPs are used for long periods or in excessive amounts, stressing the need to evaluate the effect of these particles on healthy cells.

2.3.1 Synthesis of MNPs

All studies agree on classifying methods for synthesizing MNPs, which include three main approaches: chemical approach, such as chemical reduction; physical approach, such as thermal evaporation; and biological approach, or green synthesis, where particles are synthesized using plants, bacteria, fungi, algae, and others (Ullah Khan et al., 2023). In his study, Saleh (2022) emphasized the superiority of green synthesis due to its environmental friendliness compared to other methods. Burlec et al. (2023) confirmed this, adding that using plant extracts in manufacturing is a promising environmental protection method. In contrast, a review by El-Seedi et al. (2024) indicated that green methods achieve sustainability goals but require development to achieve better productivity compared to chemical methods. Serna-Gallén & Mužina (2024) emphasized in their study that, despite the challenges of toxicity and polluting residues in chemical methods, they give producers better control over particle properties, shape, and size.

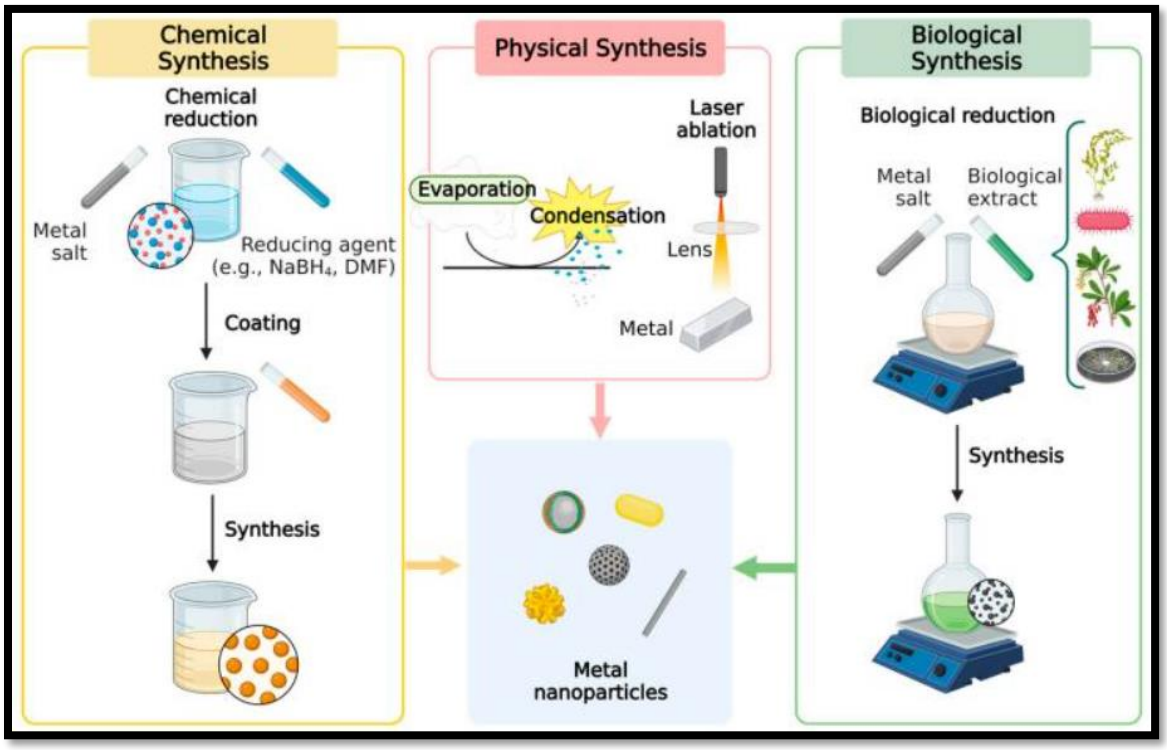

Fig. (2.3): Common synthesis techniques employed for MNPs (Burlec et al., 2023)

2.3.2 Applications of MNPs

MNPs have numerous contemporary practical applications. Saleh's study (2022) addressed their use in medicine, particularly in diagnosis and treatment, including the applications of AgNPs as antibacterial agents, stimulating complex reactions like genetic interactions, and targeting cancer cells. He also explored their role in environmental purification, such as air purification and water treatment through removing heavy metals and pollutants, a finding confirmed by El-Seedi et al. (2024) and Aminzai et al. (2024).

Burlec et al.'s study (2023) examined the ability of silver and gold NPs, in particular, to target tumors and penetrate cells with extreme precision. Shahalaei et al. described this in their study (2024) as "smart drug delivery," which contributes to treating tumors without harming healthy tissue. They also highlighted the effective role of MNPs in magnetic resonance imaging applications.

In industry, the Serna-Gallén & Mužina study (2024) indicated the role of MNPs in manufacturing sensors, batteries, and solar cells, given their distinctive electrical and optical properties mentioned above, which most studies have agreed on this role.

2.4 Methods for Analyzing Surface Roughness

With the rise of nanotechnology, it has become increasingly important to understand the surfaces of NPs and their impact on interactions and performance, to ensure they can be effectively used in various applications and fields. Different techniques are used to analyze the surface roughness of NPs, including both traditional and modern methods (Sreelatha et al., 2025; Upadhyay et al., 2023).

2.4.1 Contact Methods

Surface roughness analysis techniques began with contact methods. The most popular and widely used of these contact methods is Stylus profilometry. This is an old, simple technique in which the surface of a sample is scanned using a thin, sensitive probe. The movement of this probe across the surface allows for measuring heights and roughness, thus studying the sample's topography (Baer et al., 2013). This method produces reliable results despite its simplicity compared to more modern methods. However, it is considered specific to hard materials and metals, as it is not suitable for soft, delicate, or highly rough surfaces (Gong et al., 2018).

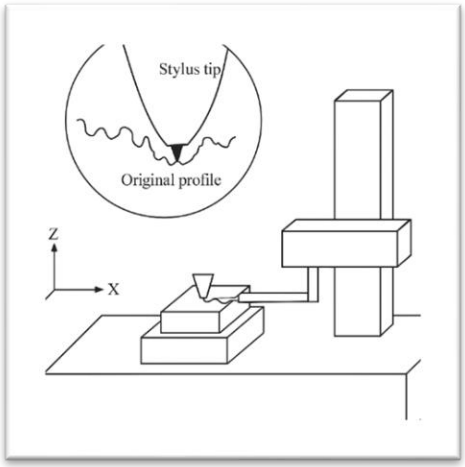

Fig. (2.4): A diagram of a stylus profilometer (Mahadeshwara, 2022)

2.4.2 Non-Contact Methods

1. Interference microscopy: One of the non-contact techniques used to study the roughness, elevations, and depressions of a sample surface, which relies on the phenomenon of optical interference. Although measuring light interferometry is not new, its integration with computers, electronics, and software has made it an effective tool in this field (Wyant, 2016).

   This technique relies on measuring surface topography using white light or a laser, which passes over the sample without contact. Interference occurs from a beam reflected off the sample surface and another from a reference mirror. This pattern is then analyzed to obtain information. This technique enables high-precision readings along with three-dimensional measurements (Groot & Lega, 2008). The most common types used are white light interferometry, phase-shifting Interferometry, and Laser Interference Microscopy. A study by Lyukshin et al. (2021) indicated that these techniques are effective but require very stable conditions due to their high sensitivity to vibrations and heat. Moreover, some types require highly reflective and flat surfaces to get useful information.
2. Scanning Electron Microscopy (SEM):

   SEM can produce high-resolution images of the sample and its topography, including roughness. This is achieved by directing a beam of electrons by acceleration voltages focused onto the sample surface. Detectors capture the backscattered and secondary electrons, which are combined and analyzed to produce a high-resolution, high-contrast topographic image of the sample surface. These images provide a reliable conception of surface roughness and can be processed digitally or with related devices to obtain numerical values (Baer et al., 2010; Mohammed & Abdullah, 2019).

   SEM is distinguished by its lack of a tip to move across the sample surface. It also enables the analysis of complex surfaces, producing results that reveal fine details of the sample surface topography with high accuracy, reaching 1 nanometer (Goodman, 2008). However, its drawbacks include potential damage to some sensitive and vital samples caused by the electron beam. Additionally, it requires a special method for sample preparation, and it prefers a high-vacuum environment to have a good result, also, it cannot provide direct numerical values, requiring subsequent analysis software (Temiz, 2022; Herrero et al., 2023).

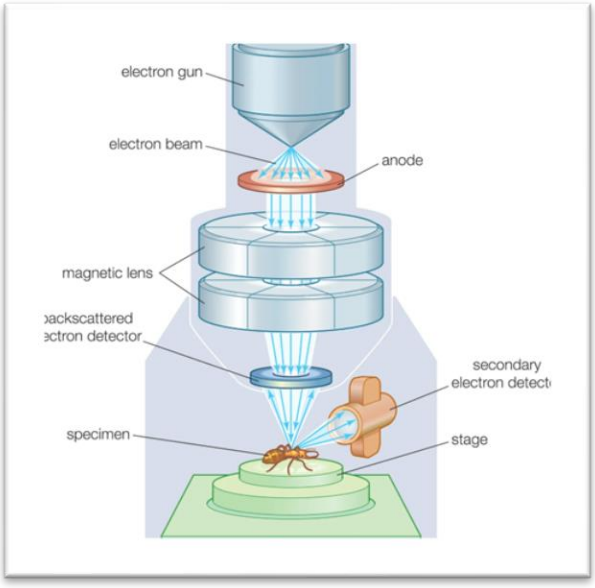

Fig. (2.5): A schematic Diagram for SEM (Joy & Ford, 2025)

3. AFM:
   Since its invention in 1986, the AFM has revolutionized the study and analysis of the behavior of surface particles, the study of interaction forces between them, and the imaging of surfaces with high-resolution three-dimensional images (Liu & Scheuring, 2013; Ishida, 2024). Not only that, but it is also a versatile instrument.
   AFM resolution reaches atomic levels, exceeding 1,000,000. In a 2007 study, Sugimoto et al. used AFM to determine the chemical properties of individual atoms. The result was the ability to distinguish between lead, tin, and silicon atoms on the surface of an alloy, despite the apparent difficulty of distinguishing them due to their similar chemical properties.

This previous result demonstrated AFM's ability to image with high atomic resolution, a remarkable achievement in our time, given the urgent need to understand, study, and characterize NPs (Bellotti et al., 2022; Ishida, 2024). It has excelled in exploring the surface roughness of NPs, providing precise three-dimensional images of the sample along with direct numerical values such as the average roughness coefficient. Additionally, it lacks specific and complex operating conditions; it can be applied in various environments, including liquid, gas, or vacuum, and does not require sample coating. However, it is slower than SEM and covers smaller measurement areas (Farré & Barceló, 2012; Llorca & Farré, 2023).

Its operating principle is based on measuring the force between the pointed microscope head and the sample atoms as it moves across the sample surface, using either contact or non-contact methods. This interaction force is analyzed to obtain a highly accurate description of the surface being studied (Ul-Islam et al., 2021). This aspect will be detailed further in Chapter 4 of this thesis.

2.5 Surface Roughness Parameters

Surface roughness is characterized using numerical values to facilitate analysis, understanding, and comparison of this physical property. These numbers are surface roughness parameters,

specifically height parameters, which can be 2D (R parameters) or 3D (S parameters). R parameters will be studied according to international standards (ISO 4287, 1997; ISO 25178, 2021). According to these standards used in most studies (Gadelmawla et al., 2002; Ruzova & Haddadi, 2025). R parameters include:

- Roughness Average (Ra): One of the easiest parameters to measure, and provides a clear description of the heights. It represents the arithmetic mean of the roughness differences or deviations from the mean line (m) along the length of the assessed profile. The mathematical definition of Ra is:

$$Ra = \frac{1}{l} \int_0^l |y(x)|\, dx \qquad (2.1)$$

Where l: is the sub-length within the total length.

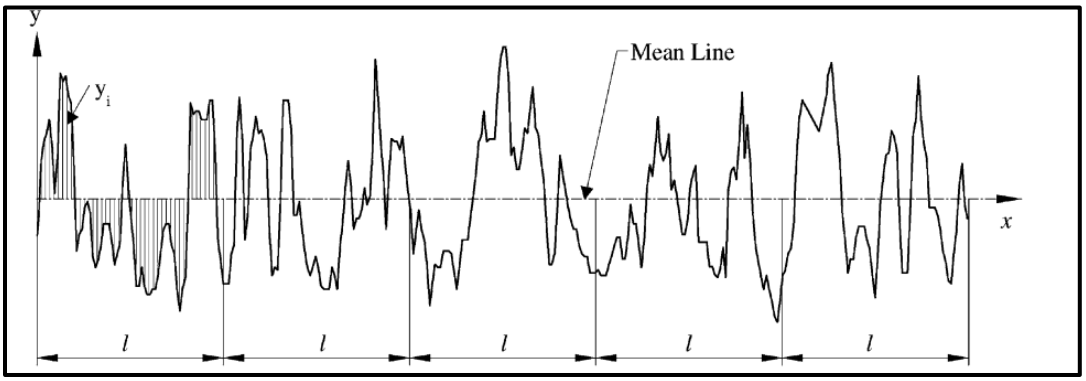

Fig. (2.6): Sampling assessment length showing l ,y, and m.

- Root mean square roughness (Rq): It is one of the most commonly used parameters for describing surface roughness. It is considered more sensitive to changes and deviations from the mean line than Ra, with a value approximately 11% higher. It represents the root mean square of the elevations along the evaluation length. The mathematical definition of Rq is:

$$Rq = \sqrt{\frac{1}{l} \int_0^l \{y(x)\}^2\, dx} \qquad (2.2)$$

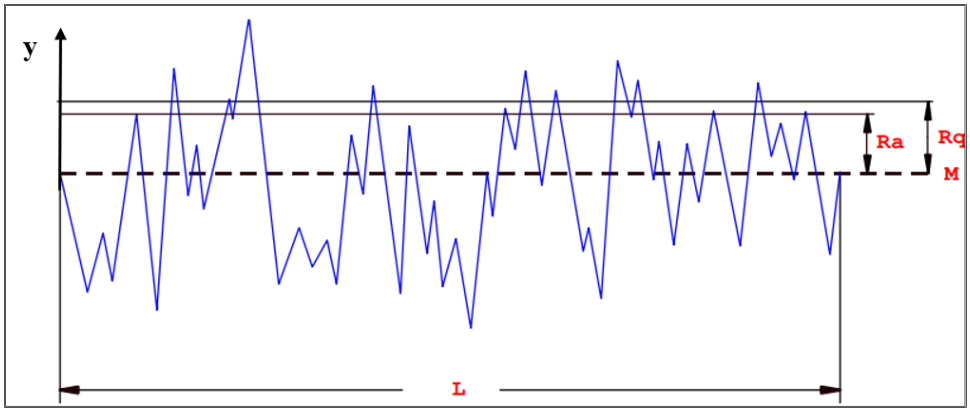

Fig. (2.7): Ra and Rq for the evaluation length.

- Maximum Profile Peak (Rp): Largest height of profile peak (above the mean line) along the evaluation length.
- Maximum Profile Valley (Rv): Largest depth of profile valley (below the mean line) along the evaluation length.
- Maximum Height (Rz): the sum of the maximum peak height and the deepest valley along the length of the sample.

$$Rz = Rp + Rv \qquad (2.3)$$

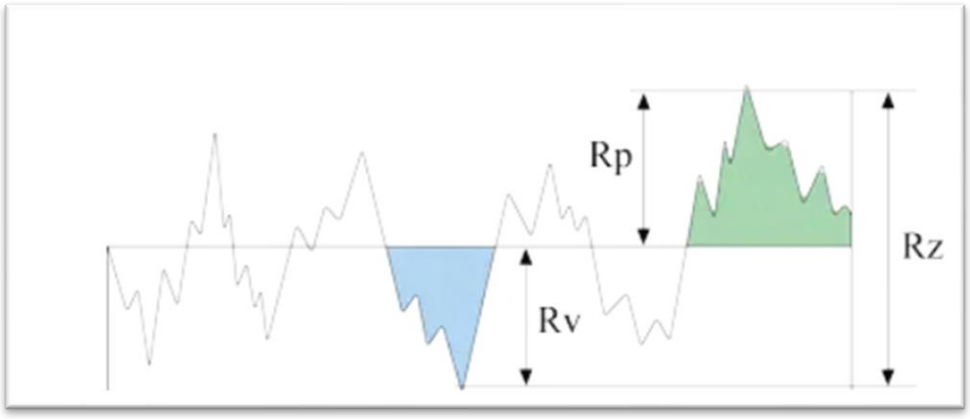

Fig. (2.8): Rp, Rv, and Rz for the evaluation length.

Chapter Three

Methodology

This chapter provides a detailed explanation of the AFM used to collect data on the surface roughness of AgNPs and its modes. It also explains the particle preparation methods and the setup used to analyze and understand the effect of these factors on the particle properties later.

3.1 Atomic Force Microscopy (AFM)

Unlike conventional microscopes that rely on light and electron beams, the AFM was invented by Binning, Quate, and Gerber in 1986 as an advanced form of scanning probe microscopy (SPM), specifically scanning tunneling microscopy (STM). While STM is limited to studying conductive materials, AFM has proven effective for investigating any type of material, including conductive and insulating materials, at the nanoscale (Binnig et al., 1986).

The microscope relies on a probe with a very sharp tip moving across the surface of a sample in different modes. The sharp tip interacts with the atoms on the sample surface due to interaction forces between them. Therefore, it is also known as the scanning force microscope (SFM). The movements of the sharp tip are recorded during the scanning process to construct a high-resolution three-dimensional image of the sample surface. AFM requires no prior sample preparation for scanning (Kyeyune, 2017; Tighe & Kiemle, 2011).

Single atoms were first seen on surfaces with the invention of AFM, which offers extremely high magnifications ranging from 100× to 100,000,000×. AFM has contributed to nanotechnology by measuring, modifying, and manipulating NPs. Its extremely high magnification enables precise measurement of surface dimensions and imaging of nanoscale particles (Nayfeh, 2008). It has also enabled nanometer-scale modifications to particles using either a pen that allows writing on surfaces, or directly depositing particles, or physically scratching them, or even using electric fields, which has developed a new lithography technique (Weng et al., 2008; Zhou et al., 2017). Finally, the microscope has also contributed to particle manipulation via a probe. Particles can be moved, rolled, and pushed to create nanoobjects, which can be harnessed to improve particle position measurement (Burger et al., 2022).

3.1.1 Components of AFM

Based on the (Vahabi et al., 2013) (Wilson & Bullen, 2006) (Kyeyune, 2017) (Giessibl, 2003) studies, the basic components of a microscope are:

1. Cantilever: A cantilever is characterized by its high flexibility, which is necessary to move on the sample surface in the desired manner. It is an arm with a very fine tip, often made of silicon or silicon compounds. Its back side is often covered with a light-reflecting material to monitor its movements.
2. Tip: It is attached to the end of the cantilever arm, and it interacts directly with the sample surface at the atomic level. Therefore, along with the cantilever, it is considered the AFM's sensitive sensor. This tip is made to be extremely fine, with a radius ranging from 2 to 20 nanometers, usually pyramidal. Imaging accuracy depends on its shape, radius, and material. For example, the sharper the tip, the greater the imaging accuracy.

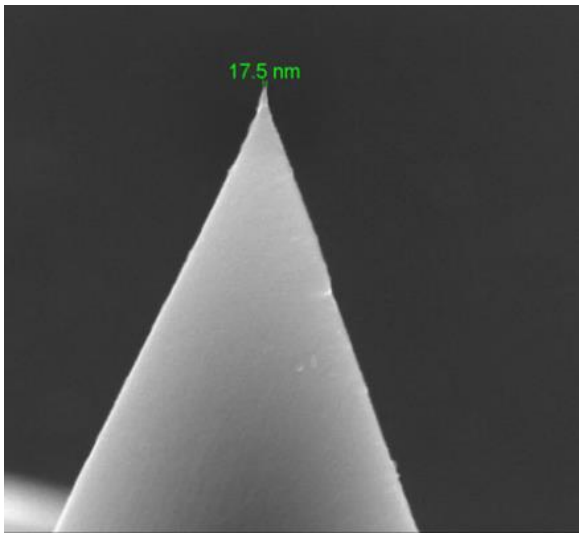

Fig. (3.1): SEM image of an AFM silicon tip (Z. Li et al., 2020).

3. Laser Source: The instrument is equipped with a laser source, directed at the back surface of the cantilever. This reflector reflects the beam onto a photodetector for analysis and reading. As the cantilever moves across the sample surface, any deflection during the measurement is measured by changes in the direction of the reflected laser beam. Thus, the cantilever deflection is read and measured.
4. Photodetector: designed to receive the laser beam reflected from the back surface of the cantilever, is highly sensitive, and is usually made as a silicon photodiode. Its importance lies in measuring the change in reflection angles resulting from the cantilever's deflection during the scanning process, which is then translated into a complete image of the sample surface. It works with the laser as a tracker, monitoring the precise movement of the cantilever.
5. Piezoelectric Scanner: It is used to control the movement of the cantilever or sample during the scanning process, allowing it to move to scan the surface in nanoscale point by point in three dimensions (X.Y.Z). It consists of motors made of piezoelectric materials, whose

geometry changes when exposed to an electrical voltage whose magnitude is determined based on signals received from the control electronics. The amount of expansion or contraction in these materials depends on the type of material and the amount of applied voltage.

Sometimes, the piezoelectric Z-actuator is classified separately for its role in controlling vertical probe motion. It operates by the same mechanism and may be located either under the sample or within the probe head.

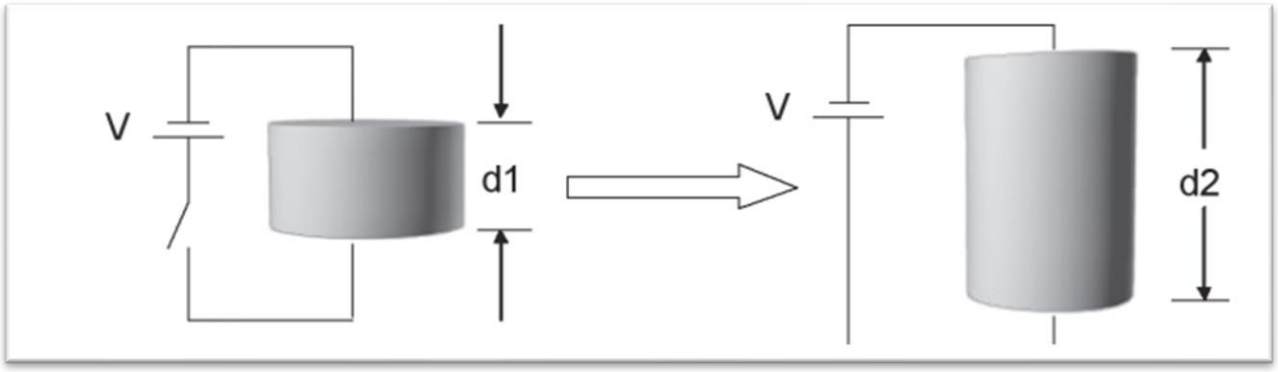

Fig. (3.2): A piezoelectric disc expands when an electric potential is applied to its sides.

6. Feedback System: It works in conjunction with the piezoelectric scanner to control the movement of the probe (cantilever and tip) on the sample surface to protect either of them from damage. It works to maintain the interaction force between the tip and the surface at a fixed, specific amount to adjust the distance between them, through continuous measurements and monitoring throughout the scanning process.
7. Sample Stage: The surface on which the sample to be imaged is placed, the stage must be designed to be stable during the scanning process and free from environmental vibrations. Its movement can be precisely controlled so that it rests below the tip of the cantilever, adapting to the sample and allowing scanning of different areas.
8. Computer and Control Electronics: The control unit supplies all microscope components with the electronic signals necessary to control their movement and elevation based on data received from the feedback system and the photodetector. This ensures successful scanning and accurate results. It also converts the results into a digital format and sends them to a computer. The computer is used to display the resulting scanning images and enables researchers to use software to process, edit, and adjust image settings.

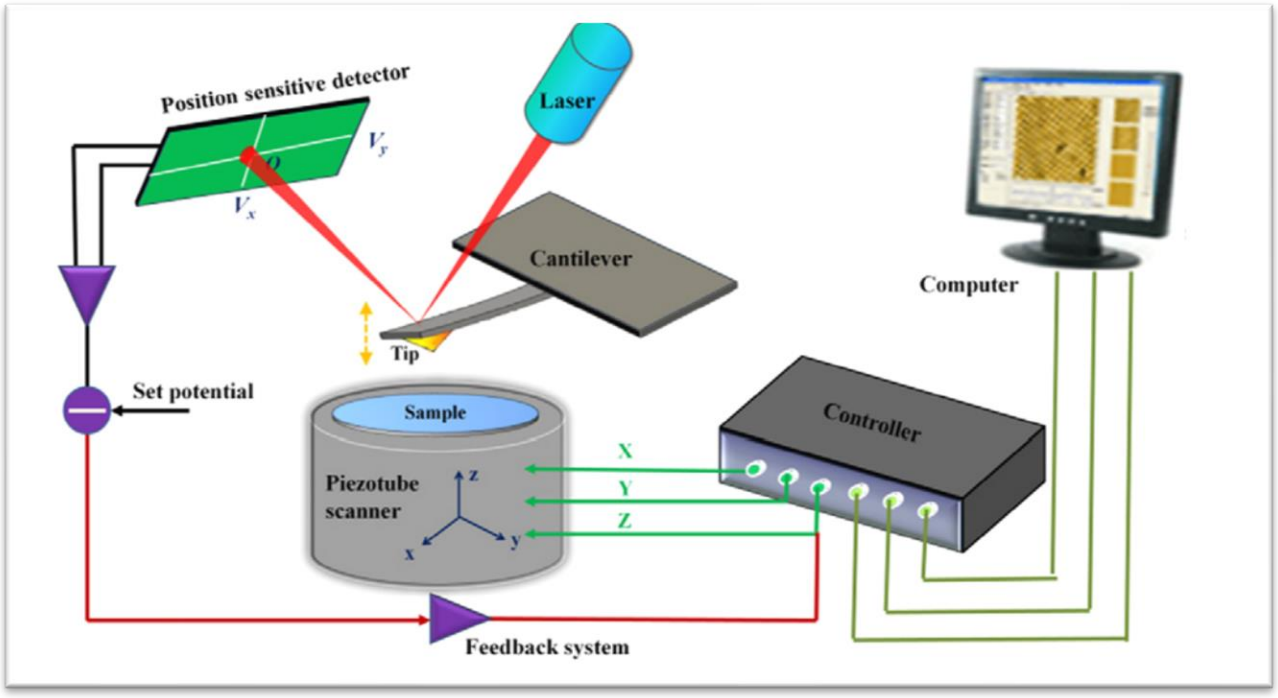

Fig. (3.3): A schematic diagram of the basic components of AFM (Guo et al., 2014)

3.2 Principle of AFM

Several studies have explained the principle of AFM and the integration of its parts together in agreement (Eaton & West, 2010; Ishida, 2024; Kyeyune, 2017; Mokobi, 2023; Triampo & Triampo, 2009; Vahabi et al., 2013; Wilson & Bullen, 2006). Based on them, the working principle is as follows:

After the sample to be studied is positioned on the stage inside the AFM, the flexible cantilever's position is carefully adjusted to prevent any sudden contact or misalignment that could damage the sensitive tip or the sample's surface and to ensure the highest possible measurement accuracy. The scanning process then begins, with the cantilever's sharp tip moving over the sample surface, tracing its atomic topography. Differences in height and depression at the atomic level lead to subtle deviations in the arm. However, the fundamental principle governing the correct movement of the cantilever, despite the varying surface topography, is the interaction forces between the tip and the sample surface. These forces (such as van der Waals forces) form the physical basis that AFM relies on for scanning and signal generation. This movement can be likened to that of an elastic spring affected by compressive or retractive forces. The cantilever's deflection is directly related to the applied force, and Hooke's law governs it as below:

$$F = -k \, . \, x \qquad (3.1)$$

Where: F= Force, k= spring constant, x= cantilever deflection

This means that the amount of interaction force between the surface and the tip depends on the deflection of the cantilever and its spring constant (i.e., its stiffness). This underscores the importance of calibrating and adjusting the cantilever before scanning to suit the sample.

Continuing AFM's operating principle, this scanning process and the cantilever's deviations require a detection system to record and analyze them to form the final image. Typically, a laser beam is directed at the cantilever's reflective-coated back surface. The laser light is reflected by a highly sensitive photodiode detector that measures the smallest changes. This detector, in turn, measures and records the angles of deflection resulting from the cantilever's deviations. This data is then converted into digital coordinates that are computer-processed to create a 3D topographic map with nanometer resolution of the sample surface.

The feedback system plays a pivotal role throughout the scanning process. Its performance is integrated with the cantilever, which is affected by interaction forces. After detecting its movement using the laser and photodetector, the feedback system analyzes it and sends electrical signals to the control unit, which then sends corrective commands to the piezoelectric actuator responsible for 3D movement (X, Y, Z) to maintain the distance according to the operating mode.

3.3 AFM modes

The AFM is operated in different modes to extract information from the sample. These modes are classified based on the interaction of the probe with the sample. The appropriate mode is chosen based on several criteria, including the nature of the sample, sensitivity to certain forces, and the experimental environment (Rana et al., 2017).

3.3.1 Contact Mode

When used in this mode, the microscope is in its simplest operating position, with the cantilever in direct physical contact with the specimen throughout the scanning process. It is adjusted so that the tip touches the sample surface. The cantilever moves above the surface at a fixed height under the influence of a constant force. Because it is affected by friction and adhesion forces, this position is suitable for samples with rough, hard surfaces. Its drawbacks include damage or distortion of soft samples, such as tissue (Eaton & West, 2010; Kyeyune, 2017).

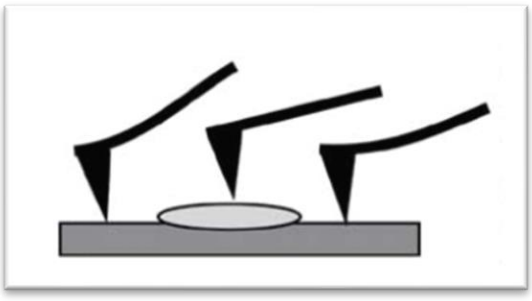

Fig. (3.4): Contact mode for AFM (Veerapandian & Yun, 2009).

In this situation, direct contact occurs between the probe tip and the sample surface, leading to the emergence of short-range repulsive forces resulting from the overlap of electron clouds between

the probe atoms and the sample atoms. This overlap is explained by the Pauli exclusion principle, which prevents the presence of two electrons in the same quantum state, resulting in a strong repulsive force known as the Pauli repulsive force. These forces can be represented using the repulsive part of the Lennard-Jones potential, which is used to estimate the behavior of interatomic forces (Giessibl, 2003; Israelachvili, 2011). The relationship between the force and the distance between the tip and the sample is:

$$F_{\text{repulsive}}\, \alpha\, \frac{1}{r^{13}} \qquad (3.2)$$

Where r = the distance between the tip and the sample.

3.3.2 Tapping Mode

Or intermediate contact, between contact and non-contact modes. In this mode, the cantilever moves near the sample surface during scanning, in intermittent contact. This means it taps the sample evenly and continuously, eliminating the effects of friction forces and others. Scanning is performed while maintaining the cantilever's motion at a constant frequency and amplitude, close to its resonant frequency. The feedback system effectively maintains the constant vibration amplitude necessary for this mode. This mode is effective for soft and biological samples, but it is slower than contact mode (Putman et al., 1994; Wilson & Bullen, 2006).

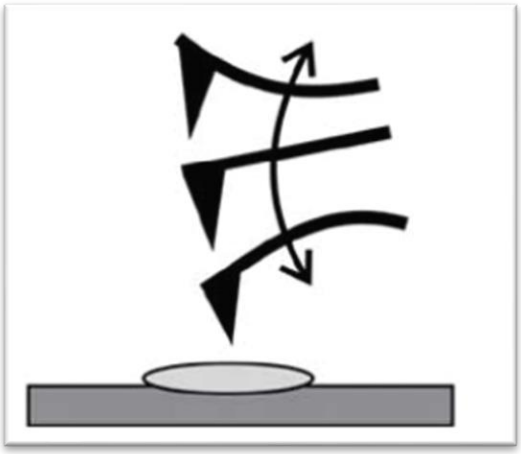

Fig. (3.5): Tapping mode for AFM (Veerapandian & Yun, 2009).

During the scanning process, the cantilever is set to vibrate vertically above the sample surface near its natural frequency, also known as the resonant frequency. This is the frequency at which the object vibrates with its maximum amplitude. Any change in the forces between the tip and the surface results in a change in the resonant frequency or vibration amplitude. This change is monitored for analysis and converted into a 3D image (Rana et al., 2017).

3.3.3 Noncontact Mode

In this mode, there is no direct contact between the cantilever tip and the sample surface. Instead, the cantilever moves at a nano fixed distance above the surface, vibrating at a frequency close to its resonant frequency. The forces interacting between the tip and the surface atoms are relatively weak, attractive forces, primarily van der Waals forces. Therefore, under some measurement conditions, a thin layer of adsorbed water molecules forms on the sample surface and also on the tip. This increases the complexity of the scanning process and affects the accuracy of measurements, making this mode less accurate. The acting forces cause subtle changes in the frequency of the cantilever and, consequently, its movement. These changes are monitored using a detection system, which can be used to construct an accurate image of the sample surface topography without causing damage (Giessibl, 2003; Vahabi et al., 2013).

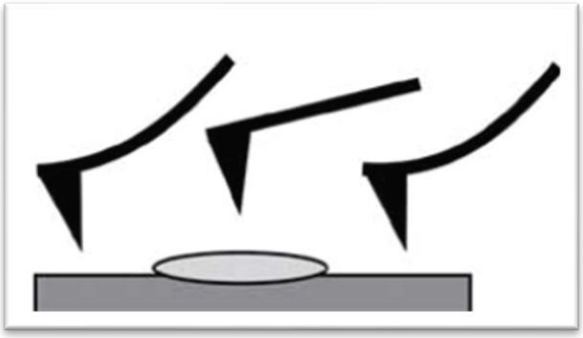

Fig. (3.6): Noncontact mode for AFM (Veerapandian & Yun, 2009).

Attractive van der Waals forces decrease rapidly with increasing distance, but they are effective at small nanoscale distances. Electrostatic forces can also appear during scanning when there are surface charges or a potential difference between the probe's tip and the sample (Israelachvili, 2011). Attractive van der Waals forces can be expressed using the following relationship:

$$F_{vdW} = -\frac{A.R}{6D^2} \qquad (3.3)$$

Where:

F_{vdW}: Attractive van der Waals force.

A: Hamaker constant, a material constant that depends on the tip's and the sample's material.

R: Tip radius

D: Distance between the tip and the sample.

*The negative sign in the equation indicates that the force is attractive.

3.4 Sample Preparation and Experimental Setup

3.4.1 Sample Preparation

Based on the thesis's objectives, AgNPs synthesized by one of two methods, green and physical, were used to compare their effects on the surface roughness of AgNPs.

3.4.1.1 Green Synthesis

To prepare AgNPs of various sizes using the green method, Pistacia Palaestina leaf extract was used as a reducing and stabilizing agent, in addition to silver nitrate ($AgNO_3$) as a source of silver ions. Preparation began by drying and grinding the leaves, adding 35 mg of leaf powder to 350 ml of deionized water, and boiling for 30 minutes. After boiling, Whatman papers, accompanied by a 0.1-µm membrane, were used to filter the solution. The resulting solution was light yellow and stored in a refrigerator at 4°C for use in the next step.

As for $AgNO_3$, several concentrations of its aqueous solutions were prepared using deionized water: 8.24 mM, 5.88 mM, 3.5 mM, and 1.18 mM. 50 mL of each concentration was taken. Thus, the samples were prepared, and the process of synthesizing AgNPs began by adding 50 mL of the plant extract dropwise to each of the $AgNO_3$ concentrations.

In the next step, each resulting mixture was heated for two hours at a temperature ranging from 80 to 84°C, with continuous stirring. The completion of the heating process marked the formal production of AgNPs, indicated by the changing mixture's color to yellowish-brown, shifting towards black.

In the final step, the resulting AgNPs were separated and purified using five centrifugations, 10 minutes each, at 10,000 rpm, to ensure completely pure particles.

To verify the success of the particle synthesis and its correct properties, their shape and morphological properties were evaluated using a scanning probe microscope (SPM-9700HT, Shimadzu, Tokyo, Japan) and an X-ray diffraction device (Bruker D2 PHASER).

3.4.1.2 Physical Method

This method combines two technologies: DC magnetron sputtering and inert gas condensation. The setup includes several integrated components: a DC magnetron sputtering head with a very high-purity silver target fixed in it, and a DC source to release silver atoms. This occurs in the presence of an inert gas, Argon (Ar), which plays an active role in the sputtering process and later assists in the condensation by acting as the carrier gas. The source and deposition chambers are separated by a pressure difference to allow the NPs to pass through. Additionally, the setup includes turbo pumps and a quadrupole mass filter (QMF) used to separate the resulting particles according to their mass or size (Fig. 3.7). The entire process takes place inside an ultra-high vacuum (UHV) compatible system from Mantis Deposition Ltd., Oxfordshire, UK.

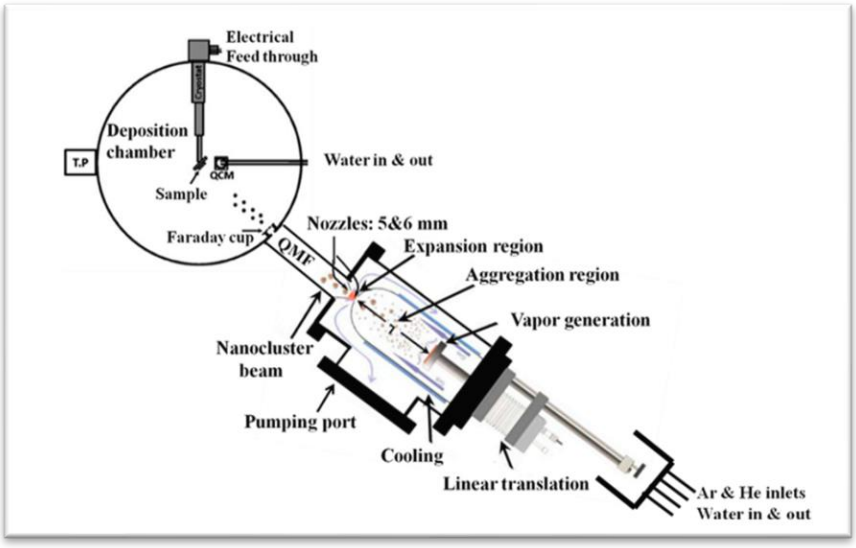

Fig. (3.7): A diagram illustrating the deposition system by magnetron Sputtering and Inert Gas condensation (Ayesh et al., 2011)

First, an inert argon gas was injected into the source chamber. Using a DC, plasma was generated inside the chamber, which facilitated the sputtering of silver atoms by colliding the ions with the silver target, releasing silver atoms.

To control the shape and size of the resulting AgNPs to the desired size, the distance between the silver target and the source chamber outlet was set to 40 mm, and a UV ratio of 0.09 was applied, values adopted from previous studies.

Then, the AgNPs condensation phase began (cluster shape), where several devices combined to achieve the desired results. To drive the condensation process evenly, a mass flow controller from Andover, MA, USA, was used to maintain an argon gas flow rate of 60 standard cubic centimeters per minute (sccm). A quartz crystal monitor (QCM) was also used to precisely monitor the deposition rate before sample stabilization. Finally, a quadrupole mass filter (QMF) was used, which operates on the principle of using both alternating current (AC) and direct current (DC) voltages to accurately separate of AgNPs by size.

For the evaluation phase of the resulting particles, a scanning prob microscopy (SPM) was used, and a Shimadzu (Kyoto, Japan) 6100 XRD instrument for X-ray diffraction analysis to confirm the crystalline structure of the material.

3.4.2 AFM Imaging

To study the surface roughness of the resulting particles at various concentrations and sizes, AFM was utilized with different tips, either standard or sharp. This approach allowed for very clear, high-resolution images of the particle surfaces.

The resulting AgNPs were mounted on a steel disc after being firmly adhered to carbon tape. Before starting the scanning process, the laser and optical sensor calibration were adjusted to accurately measure the deviation and thus obtain an optimal signal. Scanning was performed at

0.3 Hz and a resolution of 256 x 256 pixels. The device's spatial resolution was set to 0.2 nm, ensuring clear and detailed images. With green synthesis samples, the contact and tapping dynamic modes were implemented using an AFM tip from the renowned company Budget Sensor. The tip model used was the SPP-NCHR, which features a sharpness of less than 10 nm, high sensitivity, and high imaging speed, ensuring high imaging resolution.

The resulting images are in Height Trace format, which represents the true shape of the surface topography and is considered the most accurate in displaying surface topography compared to other imaging modes, such as deflection trace, which is less accurate.

3.4.3 Image Processing and Analysis

After the AFM imaging process was completed, the resulting topographic images were analyzed using the Shimadzu SPM 9700 software program. The height trace images were uploaded to the software for the needed processing.

The processing steps included smoothing and refining the surface image using *Line fit* from *Flatten*, then adjusting the colors, noise, and lines in the image to make the image's features clearer (Fig. 3.8).

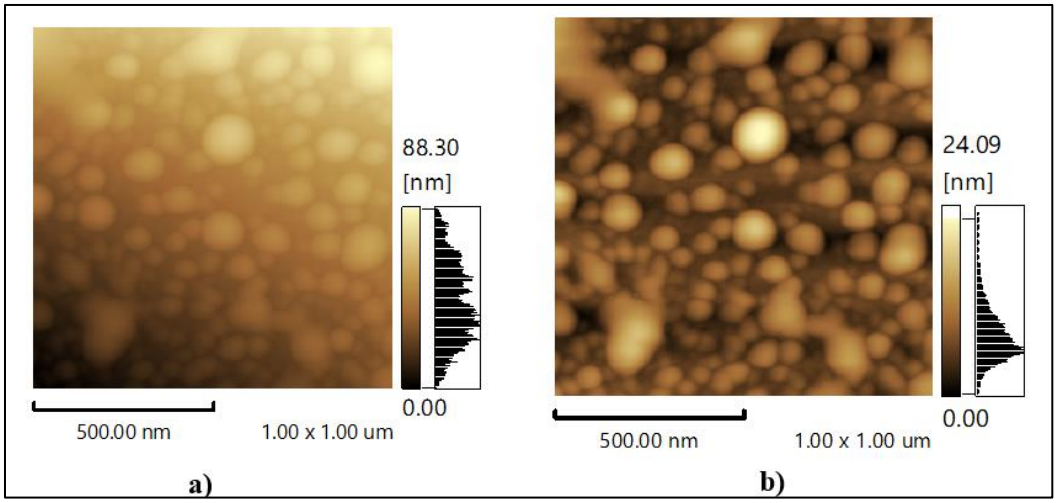

Fig. (3.8): 2D AgNPs images using AFM: **a)** before modifying. **b)** after modifying.

Quantitative data from the image, such as *Profile height* measurements and surface roughness, were then analyzed to determine the value of R parameters, especially Ra and Rq, in this study (Fig. 3.9).

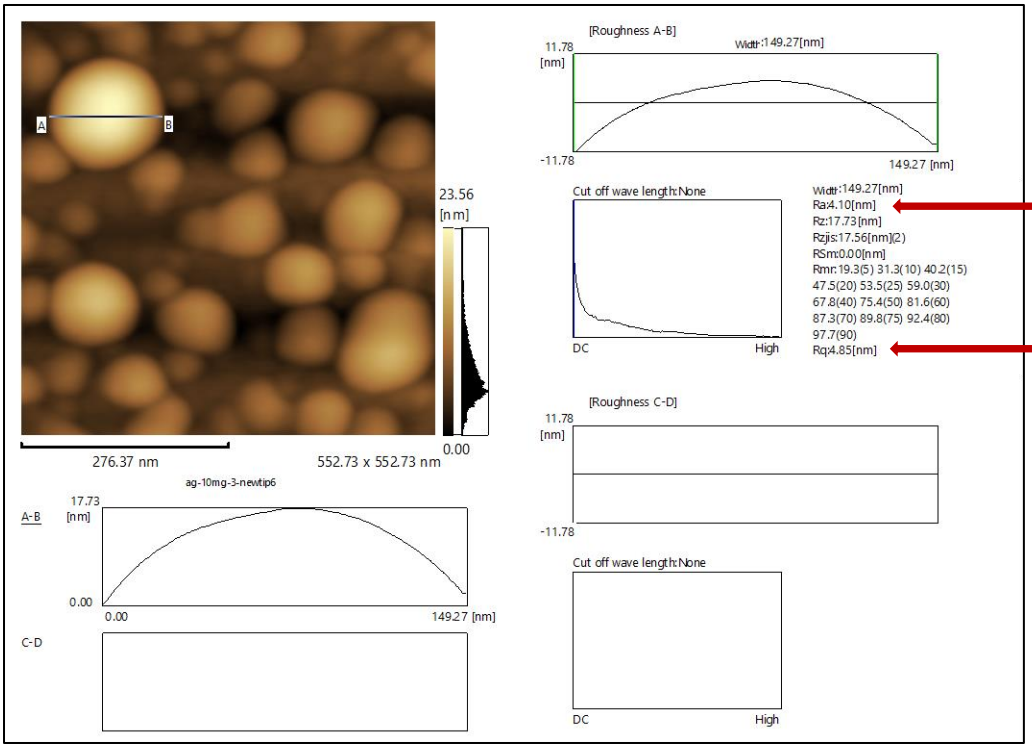

Fig. (3.9): SPM Analysis interface of AgNPs image, shows R parameters and others.

AFM can provide either 2D images or 3D images of the sample. Both images can be analyzed to calculate roughness parameters and to get a visual idea of the surface roughness (Fig. 3.10).

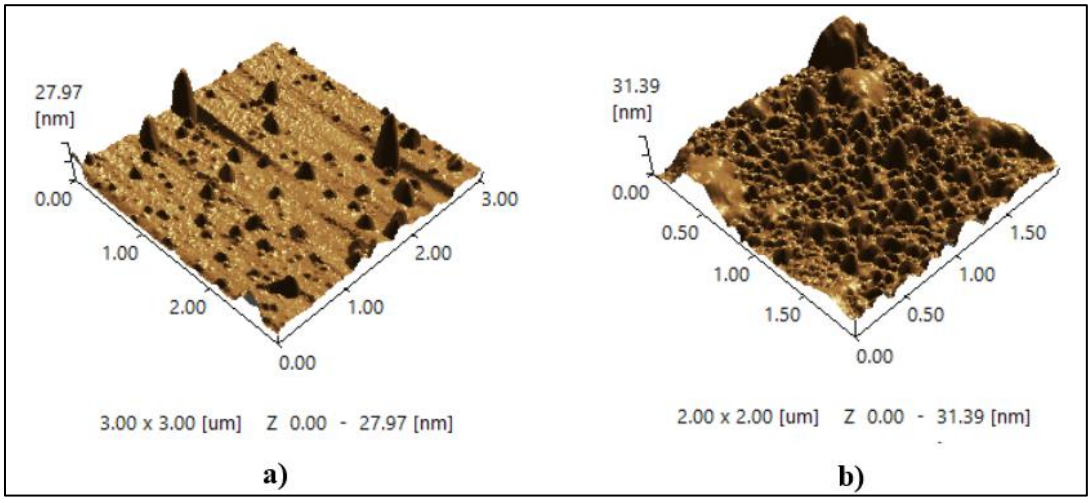

Fig. (3.10): 3D AFM images of AgNPs samples at different concentrations: **a)** 30 mg/50 mL, **b)** 10 mg/50 mL, obtained by SPM software.

Chapter Four

Results and Discussion

Factors Affecting Surface Roughness of NPs: An Analytical Study

This chapter presents the study results obtained by implementing the procedures described before. These results aim to evaluate and understand the surface roughness property of AgNPs and the extent to which it is affected by criteria identified in the study objectives, which include: the size of NPs and their relationship to surface roughness, the extent to which the surface roughness of the resulting samples is affected by the concentration of NPs during the synthesis process, a comparison of the surface roughness values resulting from using different types of tips in AFM imaging (standard and sharp), and finally an analysis of the effect of different synthesis methods on the surface roughness of the resulting NPs, between physical and green methods.

Understanding how these factors influence the surface roughness is crucial, given the role this property plays in determining the behavior of NPs at the physical and chemical levels, particularly in applications related to catalysis, bioreactivity, and delivery. Therefore, surface roughness analysis is a pivotal step in evaluating the functional performance of NPs under various conditions (Darwish & Helmy, 2022).

Section 1: Variation in Surface Roughness Correlated with NPs Size

One of the most important physical factors affecting the properties of NPs is their size. During the synthesis process, particles of different shapes, sizes, and diameters are produced due to the influence of the synthesis conditions, such as concentration and temperature etc (Baer et al., 2013). Considering NMs and the aggregation of NPs of different sizes to form them, this will significantly affect their surface properties, particularly roughness. Hence, the importance of studying and analyzing this factor to gain a deeper understanding of one of the factors influencing surface roughness, and thus using NPs more effectively in applications.

Based on the objective of studying the correlation of surface roughness contrast with the size of NPs, topographic measurements and values were obtained to calculate the Ra and Rq of the surface

of some AgNPs after scanning and analyzing them as mentioned in the methodology. The results were shown in a picture for the sample Fig. (4.1), followed by Table (4.1) showing the calculated parameters and a graph of the values in Fig. (4.2) as follows:

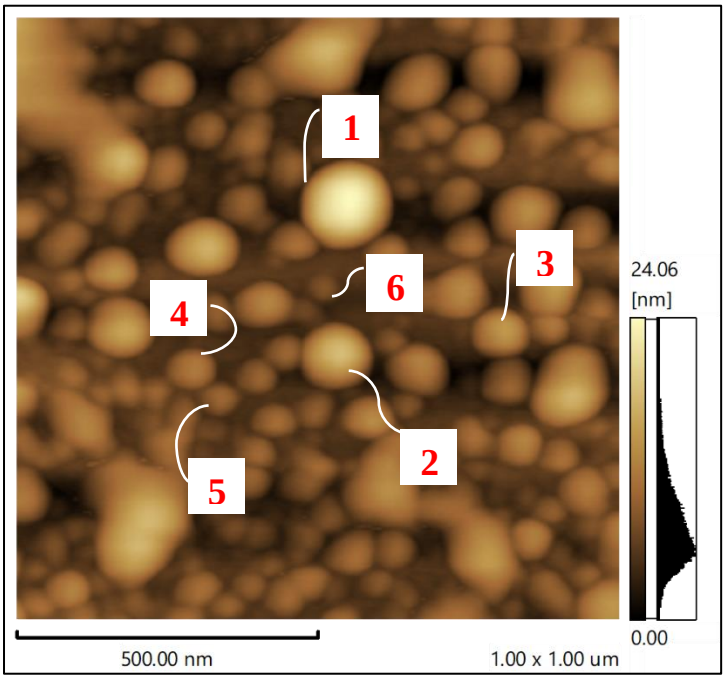

Fig. (4.1): An AFM height trace image for AgNPs shows particles of different sizes.

Particles of clearly distinct sizes were selected within the sample, and their values were recorded. The particles are arranged in the table below in ascending order from smallest to largest.

Table 4.1: Ra and Rq for different sizes of AgNPs.

# of Particle (Asc. based on size)	A-B Profile Height (nm)	Ra (nm)	Rq (nm)
Particle 1	2.53	0.64	0.74
Particle 2	3.37	0.86	1
Particle 3	5.98	1.45	1.71
Particle 4	8.78	2.02	2.39
Particle 5	10.58	2.76	3.24
Particle 6	17.73	4.1	4.85

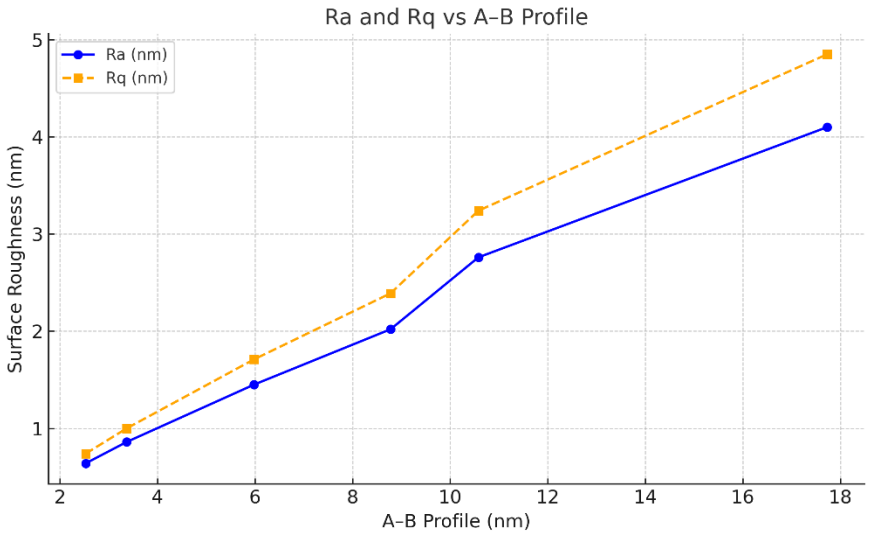

Fig. (4.2): Graph showing the relationship between NPs size (A–B Profile) and Ra and Rq.

The data in the table clearly and noticeably show that the larger the nanoparticle size, the higher the roughness coefficient values (Ra, Rq). This proves that there is a relationship between particle size and surface nature. The relationship between particle size and surface roughness is a direct, linear relationship.

Note: A–B Profile refers to the height of the cross-section measured on the AFM image and does not represent the full particle size.

In a study published by Kumar in 2021, the combined effect of NPs size and surface roughness on the heat transfer performance of nanofluids was investigated. The results showed that increasing the NPs size increases surface roughness, which significantly affects heat transfer performance.

In another study by Athauda et al. (2013), the effect of depositing silica NPs of different sizes, with diameters ranging from 7 to 40 nanometers, on a glass surface was examined. The results showed that depositing larger particles on top of smaller particles increased surface roughness, which further enhanced their hydrophobic properties. This highlights the importance of controlling the size of NPs to control surface roughness and wettability.

This is consistent with the findings in this study, which show a direct relationship between particle size and surface roughness. It also confirms the significant impact of surface roughness on the physical and chemical properties of materials.

This relationship between NPs size and surface roughness can be explained by the fact that larger NPs contribute to more prominent surface topography, which increases the variation in surface heights and depressions of the sample. This effect may result from the accumulation of larger particles on the surface of the material, leading to an increase in the overall surface roughness.

Section 2: Dependency of Surface Roughness on the Concentration of NPs During Synthesis

This section studies the effect of NP concentration on surface roughness during the synthesis process. Surface roughness values of 4 samples with different nanoparticle concentrations (10, 30, 50, and 70) mg/50 mL, referred to as NP-10, NP-30, NP-50, and NP-70, respectively, are compared.

The roughness coefficients were calculated for several particles from each concentration as follows:

First: AgNPs with NP-10 concentration:

The AFM image of NP-10 of AgNPs is shown in Fig. (4.3), followed by Table (4.2) showing the calculated parameters.

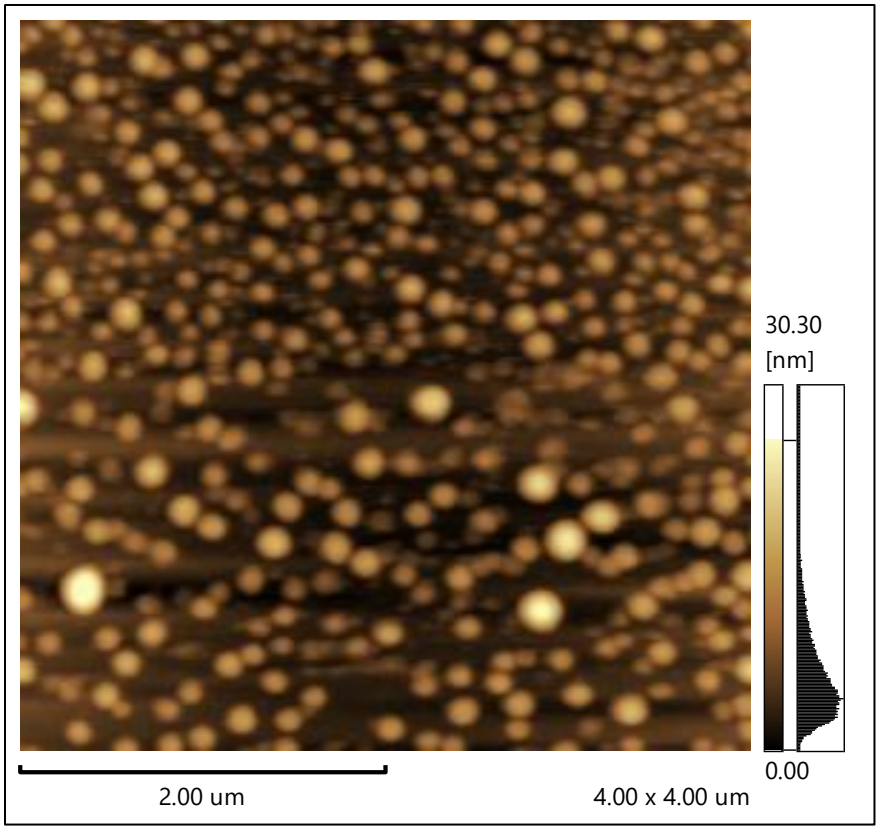

Fig. (4.3): An AFM image for AgNPs at NP-10 concentration modified by SPM software.

Table 4.2: Ra and Rq for AgNPs at NP-10 concentration.

# of Particle	Ra (nm)	Rq (nm)
Particle 1	5.59	6.46
Particle 2	6.22	7.2
Particle 3	5.08	5.88
Particle 4	4.85	5.61
Average	**5.435**	**6.287**

Second: NP-30 concentration:

The AFM image at NP-30 of AgNPs is shown in Fig. (4.4), followed by Table (4.3) showing the calculated parameters.

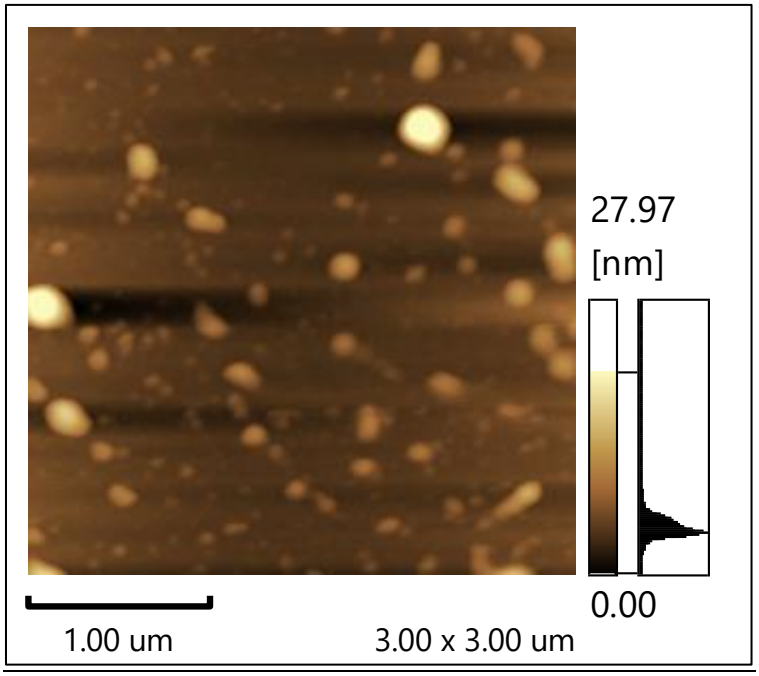

Fig. (4.4): An AFM image for AgNPs at NP-30 concentration modified by SPM software.

Table 4.3: Ra and Rq for AgNPs with 30 M concentration.

# of Particle	Ra (nm)	Rq (nm)
Particle 1	7.08	8.23
Particle 2	2.88	3.38
Particle 3	3.79	4.41
Particle 4	2.46	2.85
Average	**4.05**	**4.71**

Third: NP-50 concentration:

The AFM image of NP-50 concentration of AgNPs is shown in Fig. (4.5), followed by Table (4.4) showing the calculated parameters.

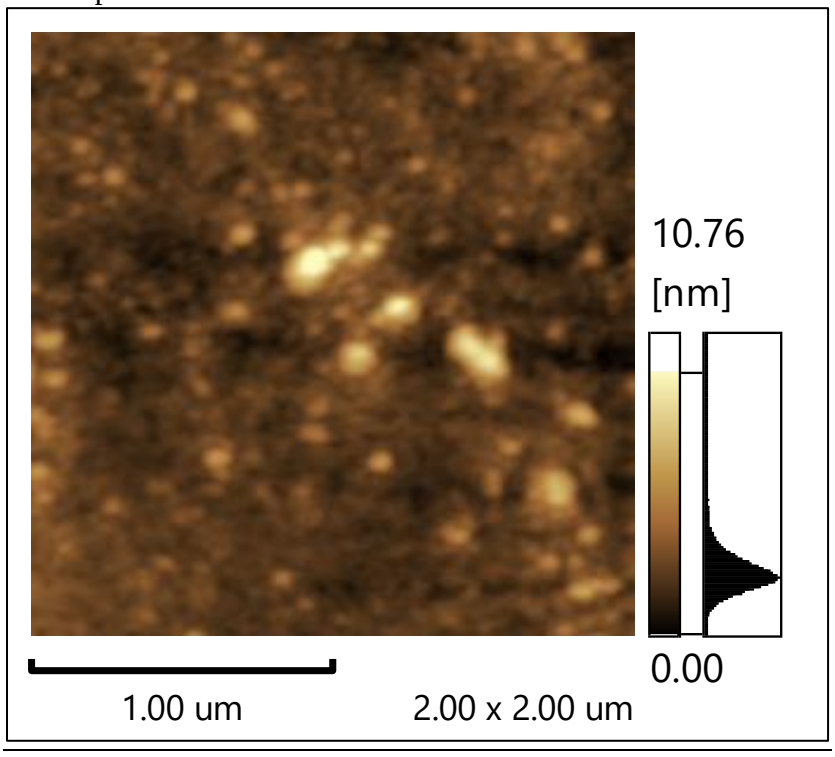

Fig. (4.5): An AFM image for AgNPs at NP-50 concentration modified by SPM software.

Table 4.4: Ra and Rq for AgNPs at NP-50 concentration.

# of Particle	Ra (nm)	Rq (nm)
Particle 1	1.83	2.09
Particle 2	0.91	1.04
Particle 3	1.29	1.5
Particle 4	0.73	0.84
Average	**1.19**	**1.36**

Fourth: NP-70 concentration:

The AFM image of NP-70 concentration of AgNPs is shown in Fig. (4.6), followed by Table (4.5) showing the calculated parameters.

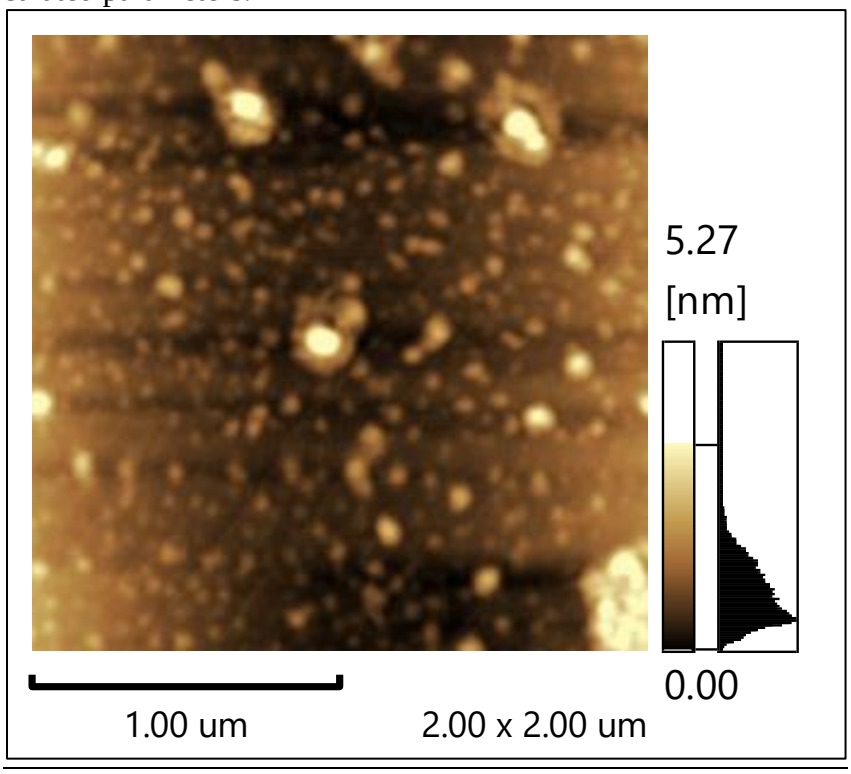

Fig. (4.6): An AFM image for AgNPs at NP-70 concentration modified by SPM software.

Table 4.5: Ra and Rq for AgNPs at NP-70 concentration.

# of Particle	Ra (nm)	Rq (nm)
Particle 1	0.75	0.87
Particle 2	0.91	1.04
Particle 3	0.73	0.84
Particle 4	0.55	0.63
Average	**0.735**	**0.845**

Comparison between 4 concentrations:

Now, Table (4.6) shows the Average value of Ra and Rq for 4 concentrations to compare them, followed by a graph, Fig. (4.7):

Table 4.6: A comparison between Ra and Rq for 4 concentrations:

Concentration	Avg. Ra (nm)	Avg. Rq (nm)
NP-10	5.435	6.287
NP-30	4.050	4.710
NP-50	1.190	1.360
NP-70	0.735	0.845

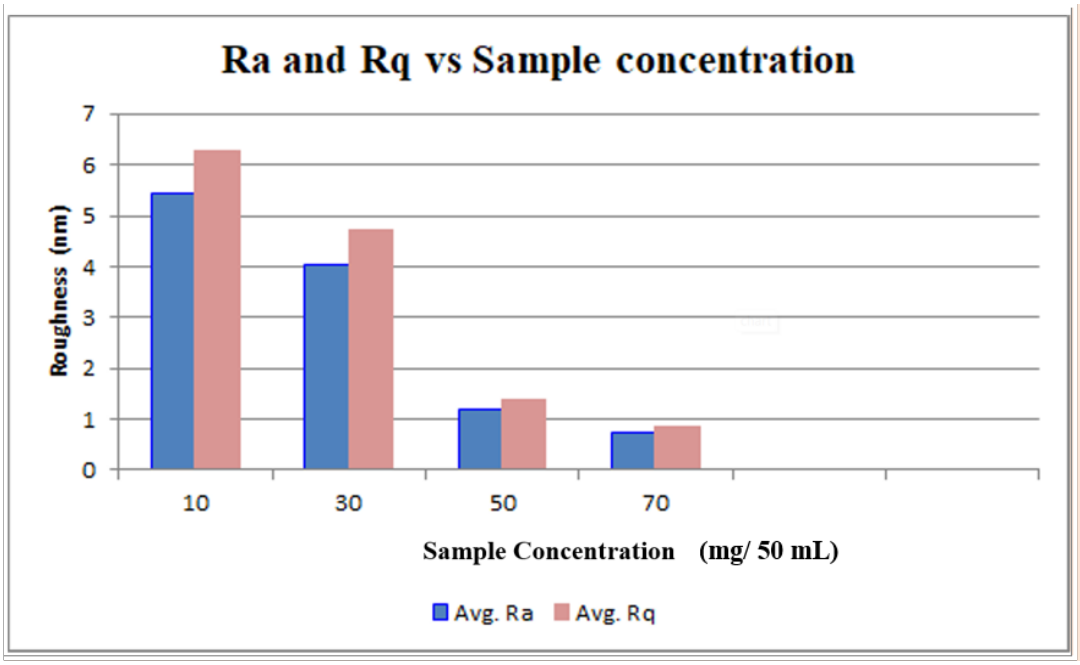

Fig. (4.7): A graph chart shows Ra and Rq for NP-(10, 30, 50, 70) AgNPs concentrations.

The results show an inverse relationship between the concentration ratio and the surface roughness of AgNPs. As the concentration ratio during synthesis increases, the values of the surface roughness parameters decrease significantly, and this result appears for all concentration ratios.

The research results are consistent with a study conducted by Montes Ruiz-Cabello et al. (2023), in which water-resistant steel surfaces were prepared by depositing zinc (ZnO) NPs at different concentrations. The results showed that surface roughness increased at low to medium concentrations, but began to decrease at higher concentrations. This was explained by the fact that the excessive accumulation of particles led to the formation of a more homogeneous and regular layer on the surface, which reduced the differences in heights and depressions, resulting in lower roughness values.

Also, in a recent study conducted by Firouz et al. (2024), the effect of adding AgNPs at different concentrations (100, 200, 350, and 500 mg/ml) to porcelain used in dental applications was evaluated. The results showed that increasing the NPs concentration led to a significant decrease in surface roughness parameters Ra and Rq. This decrease was explained by the fact that the NPs at higher concentrations helped fill surface gaps and were distributed homogeneously, leading to a reduction in topographical irregularities on the material's surface.

Section 3: Comparison of Surface Roughness Measurements Using Different AFM Tips: Standard and Sharp

AFM tips are one of the most important factors that influence the accuracy of the resulting measurements, especially when analyzing surface properties such as surface roughness measurements. This tip, located at the end of the cantilever, is manufactured with a very small

radius, which can reach less than 10 nanometers, to enable precise interaction with the sample surface (Bhushan, 2010).

AFM tip types vary based on the material (such as silicon or silicon nitride), tip shape (spherical, pyramidal, or very sharp), as well as its hardness, spring constant, and degree of sharpness. The tip is selected based on the sample type, the nature of the surface, and the operating mode used. Common types include: Standard tips, these tips typically have a radius of 8–10 nm, and Sharp tips, which are sharper, with a radius of less than 5 nm, allowing them to reveal very fine surface details. They are particularly used for analyzing sample surfaces with high nanoscale resolution, which helps in obtaining accurate R parameter calculations (Bhushan, 2010; Cappella & Dietler, 1999).

This section aims to study the effect of using two types of tips: standard and sharp, in the process of measuring the surface roughness of AgNPs, and the extent of the tip's influence on the measurement accuracy. The results are shown in Fig. (4.8), followed by Table (4.7).

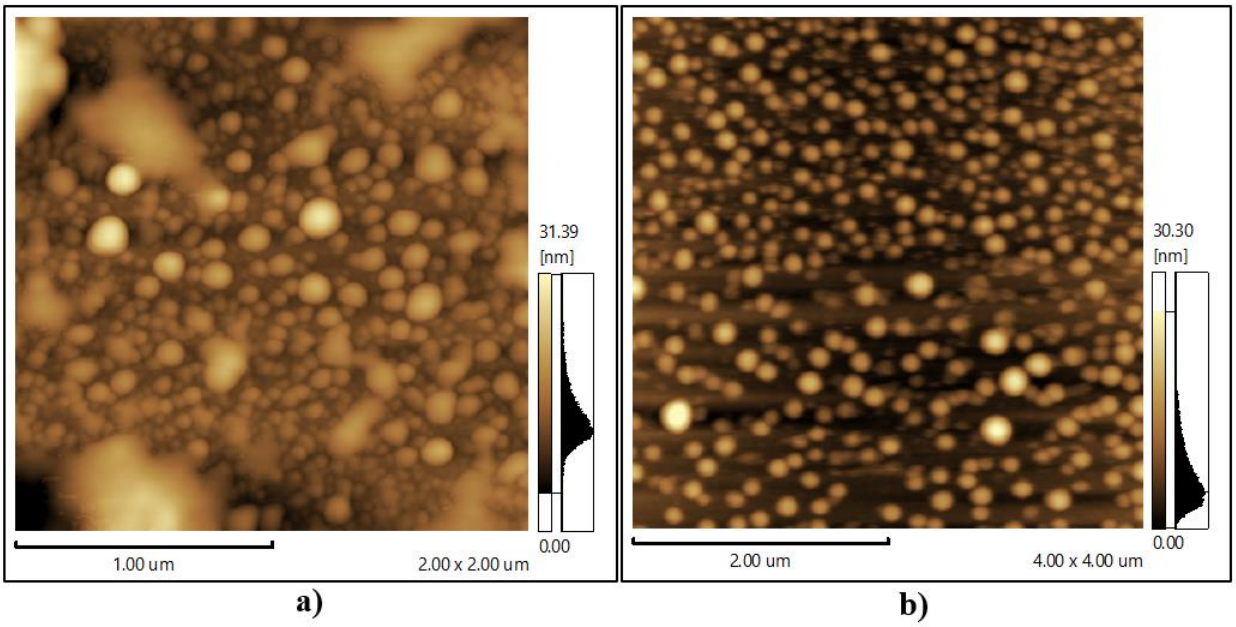

Fig. (4.8): AFM images of AgNPs by different tips: a) Standard, b) Sharp.

Table 4.7: Ra and Rq of sharp and standard tip:

# of Particles	Standard Tip		Sharp Tip	
	Ra (nm)	**Rq (nm)**	**Ra (nm)**	**Rq (nm)**
Particle 1	4.39	5.20	5.59	6.46
Particle 2	4.26	5.22	6.22	7.20
Particle 3	2.93	3.52	5.08	5.88
Particle 4	2.87	3.44	4.85	5.61
Average	**3.61**	**4.345**	**5.435**	**6.287**

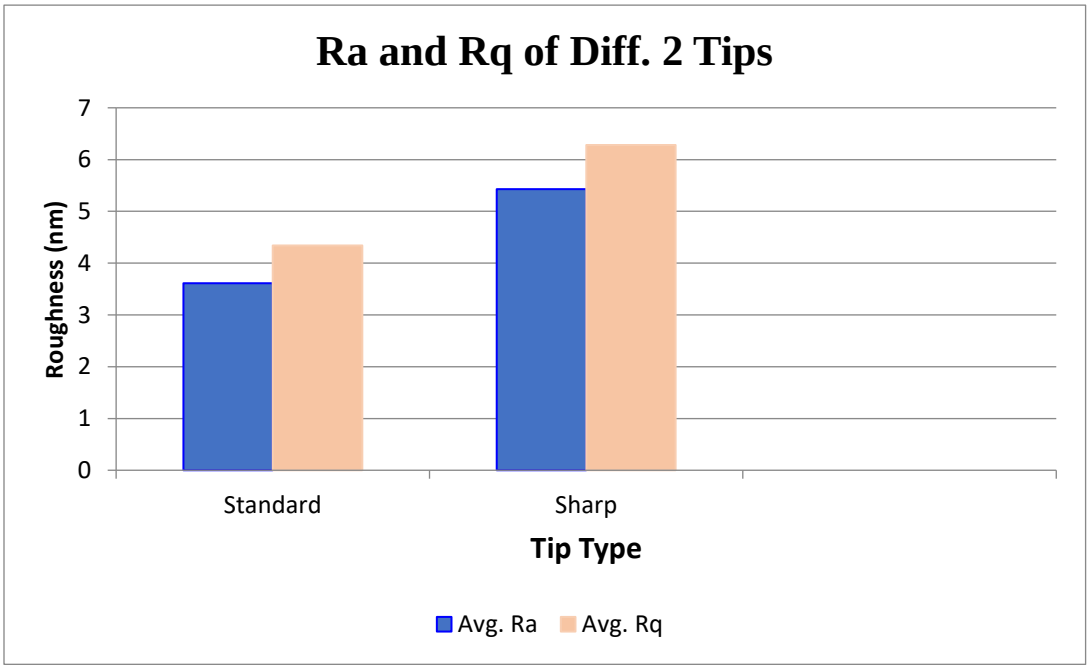

Fig. (4.9): A graph chart shows Ra and Rq for standard and sharp tips.

The sharp tip showed greater surface roughness measurements than the standard tip, proving that surface roughness accuracy measurements are affected by the type of AFM's tip during scanning. The sharper the tip, the more accurate the measurements.

This result is consistent with several studies. For example, in a study conducted by Sedin & Rowlen (2001), the effect of the tip size on surface roughness measurements was evaluated using tips of different sizes. The results showed that using smaller radius (sharper) tips resulted in higher and more accurate roughness values. This was explained by the fact that sharper tips are better able to track fine surface details and reduce the probability of ignoring some fine details on the sample surface.

This result is supported by a recent study conducted by Xu & Leng (2024), in which sharp AFM tips were used to scan nanostructures and their effect on roughness measurements was evaluated. The results showed that sharper tips provide higher-quality images, reduce distortions during the measurement process, and improve the accuracy of surface roughness measurements because they provide more realistic results about the surface structure.

Section 4: Influence of Synthesis Techniques on Surface Roughness, Comparing Physical and Green Methods.

The properties of NPs are greatly influenced by their synthesis method, including their surface roughness due to different growth conditions and particle aggregation mechanisms (Saadat et al., 2020). A sample synthesized by physical methods was studied in terms of its roughness with another sample synthesized by the green method to understand the effect of the method on the surface roughness.

First: Physical Method

The surface roughness of the AgNPs sample synthesized by the previously described physical method was analyzed, and its roughness parameters were measured to determine the result. The results were in Fig. (4.10), followed by Table (4.8) as follows:

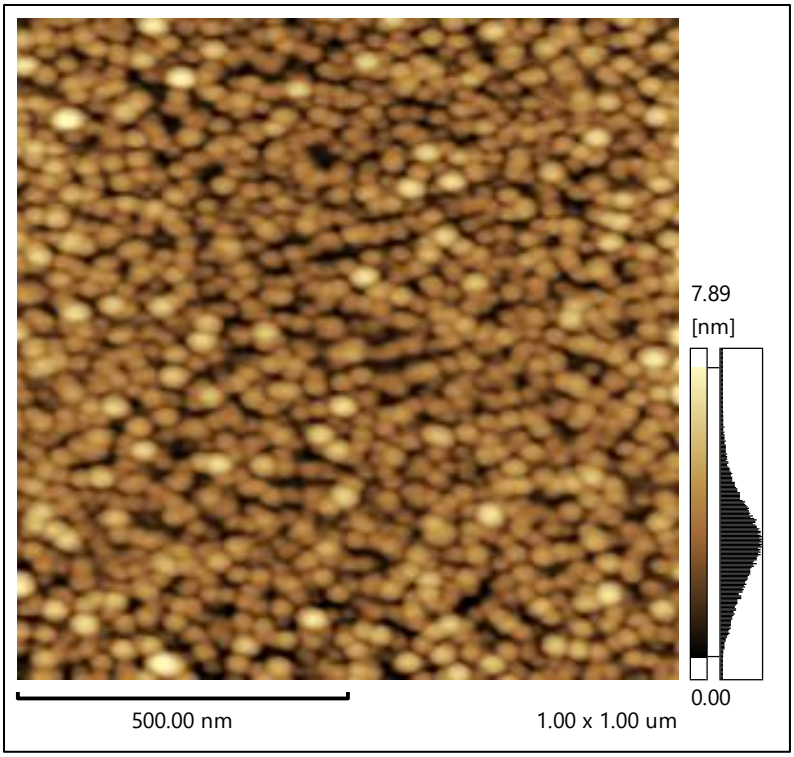

Fig. (4.10): An AFM image for AgNPs: Physically synthesized.

Table 4.8: Ra and Rq for 4 AgNPs synthesized by the physical method.

# of Particle	Ra (nm)	Rq (nm)
Particle 1	0.93	1.08
Particle 2	1.07	1.26
Particle 3	1.02	1.19
Particle 4	1.11	1.29
Average	**1.03**	**1.20**

Second: Green Method

In this section, the samples used in the concentration section were also used here. Because they were manufactured using the green method. The surface properties of the physical method were compared with values determined by the green method at two different concentrations (30 and 70 mg). Ra and Rq values for both methods are shown in Table (4.9), followed by Fig. (4.11).

Table 4.9: Ra and Rq values of AgNPs synthesized by physical and green methods.

Synthesis method		**Avg. Ra (nm)**	**Avg. Rq (nm)**
Physical method		1.03	1.2
Green method	NP-30	4.05	4.71
	NP-70	0.73	0.84

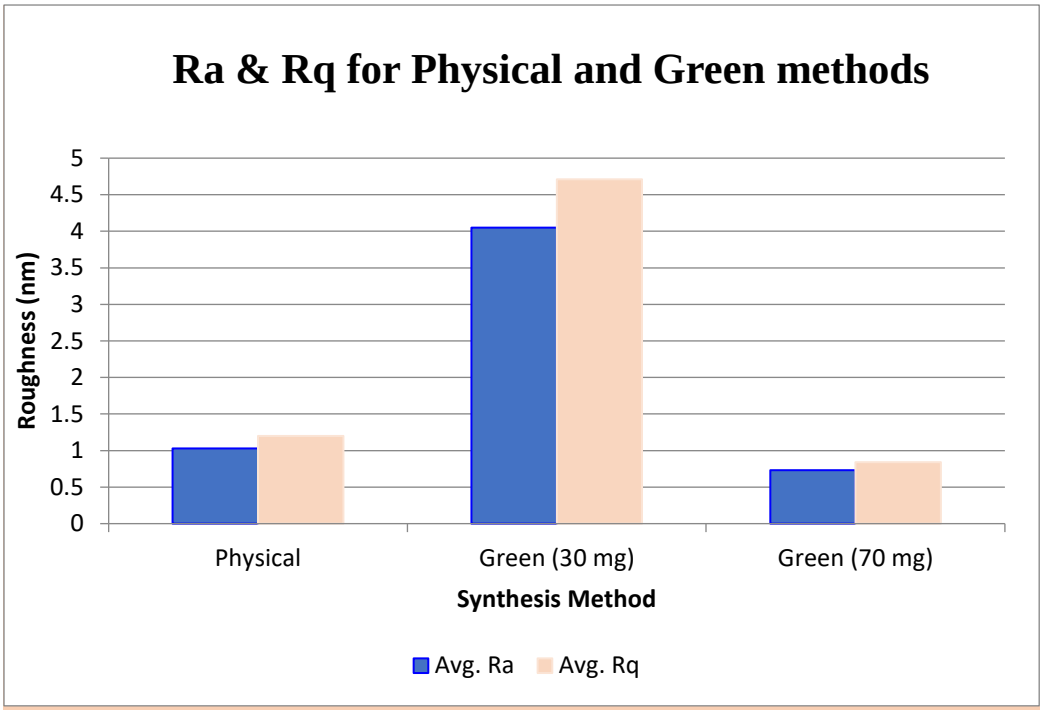

Fig. (4.11): A graph chart shows Ra and Rq for physical and green sunthesis.

A significant difference in the surface roughness of the particles was observed depending on the synthesis method. For example, AgNPs synthesized using the green method at a lower NPs concentration exhibited significantly higher surface roughness than those synthesized using the physical method, while roughness values were nearly at a concentration of 70 mg, or even slightly higher for physical AgNPs. The surface roughness of NPs synthesized using the physical method was intermediate between the two values in the green method.

This result is consistent with a study conducted by J. Singh et al. (2018), where the researchers indicated that green synthesis results in greater surface roughness. This was explained by the fact that this method at low concentrations may lead to irregular particle agglomeration due to the lack of stabilizing agents, which is reflected in the resulting increased surface roughness.

Another study by Vanlalveni et al. (2021) supported this finding, showing that particles produced by physical synthesis tend to have more uniform and less rough surfaces due to the possibility of controlling the production conditions and the resulting particles compared to the green method. On the other hand, a study by Ramesh et al. (2015) demonstrated that increasing the concentration of plant extract in green synthesis helps reduce surface roughness. This was explained by the fact that green synthesis methods at higher concentrations facilitate greater particle arrangement on the surface, thus reducing roughness. This explains why roughness values for the green method at higher concentrations are closer to those for the physical method in this study's results.

Chapter Five

Conclusions and Future Work

5.1 Conclusions

This study aimed to analyze the effect of a range of physical factors on the surface roughness of AgNPs, using AFM as the primary analytical tool coupled with a software program. The research focused on 4 variables to understand their impact on surface roughness: AgNPs size, particle concentration during the synthesis process, the type of probe tip used (sharp, standard), and the particle synthesis method (physical and green synthesis).

The results showed a direct relationship between particle size and surface roughness. The larger the particle size, the higher the surface roughness values, reflecting the influence of larger particles on the surface structure when building NMs. Conversely, an inverse relationship was observed between AgNPs concentration during the synthesis process and surface roughness. Roughness values decreased significantly as the particle concentration increased, which is explained by the more uniform coverage of the sample surface when a larger number of particles were present.

It was also found that using a sharp tip resulted in higher surface roughness values compared to standard tips, because the sharper tip's increased sensitivity to the sample's surface structure, resulting in more accurate measurements.

Finally, a comparison between the physical and green synthesis methods for preparing AgNPs revealed a clear discrepancy in roughness values. The roughness value obtained from the physical method fell between the values obtained from two different concentrations (30 and 70 mg) in the green synthesis method, and was closer to the higher concentration (70 mg), indicating that the NPs are affected by the different synthesis methods.

These results support the importance of tuning the synthesis and analysis conditions of NPs for their effective use in nanoscale applications, given their direct impact on surface properties, which play a crucial role in the performance of materials in various application areas such as medicine, sensing, and catalysis.

5.2 Future Work

Based on the results obtained in this study, several future directions can be proposed to expand our understanding of NPs surface roughness and its impact on various factors. Further studies are needed to test other synthesis methods, their impact, and to compare the results of each. Additional factors affecting the synthesis process, such as pH and temperature, needed to be studied. It is also necessary to study the different tip shapes for the device and determine the most appropriate one based on the application used for the particles.

In applications, there is a need to analyze the relationship between surface roughness and the physical and chemical properties of NPs, such as their electrical, optical, and antibacterial efficacy, to determine how roughness affects practical performance.

References

- Abass Sofi, M., Sunitha, S., Ashaq Sofi, M., Khadheer Pasha, S. K., & Choi, D. (2022). An overview of antimicrobial and anticancer potential of silver nanoparticles. *Journal of King Saud University-Science*, *34*(2), 101791. https://doi.org/10.1016/j.jksus.2021.101791
- Abbas, R., Luo, J., Qi, X., Naz, A., Khan, I. A., Liu, H., Yu, S., & Wei, J. (2024). Silver Nanoparticles: Synthesis, Structure, Properties and Applications. *Nanomaterials*, *14*(17), Article 17. https://doi.org/10.3390/nano14171425
- Abdelkawi, A., Slim, A., Zinoune, Z., & Pathak, Y. (2023). Surface Modification of Metallic Nanoparticles for Targeting Drugs. *Coatings*, *13*(9), 1660. https://doi.org/10.3390/coatings13091660
- Alagarasi, A. (2011). *INTRODUCTION TO NANOMATERIALS* (p. 76).
- Alkhalayfeh, M. A., Aziz, A. A., Pakhuruddin, M. Z., & Katubi, K. M. M. (2022). Plasmonic Effects of Au@Ag Nanoparticles in Buffer and Active Layers of Polymer Solar Cells for Efficiency Enhancement. *Materials*, *15*(16), 5472. https://doi.org/10.3390/ma15165472
- Alshehri, A. H., Jakubowska, M., Młożniak, A., Horaczek, M., Rudka, D., Free, C., & Carey, J. D. (2012). Enhanced Electrical Conductivity of Silver Nanoparticles for High Frequency Electronic Applications. *ACS Applied Materials & Interfaces*, *4*(12), 7007–7010. https://doi.org/10.1021/am3022569
- Altammar, K. A. (2023). A review on nanoparticles: Characteristics, synthesis, applications, and challenges. *Frontiers in Microbiology*, *14*, 1155622. https://doi.org/10.3389/fmicb.2023.1155622
- Amendola, V., & Meneghetti, M. (2009). Laser ablation synthesis in solution and size manipulation of noble metal nanoparticles. *Physical Chemistry Chemical Physics*, *11*(20), 3805. https://doi.org/10.1039/b900654k
- Aminzai, M. T., Yildirim, M., & Yabalak, E. (2024). Metallic nanoparticles unveiled: Synthesis, characterization, and their environmental, medicinal, and agricultural applications. *Talanta*, *280*, 126790. https://doi.org/10.1016/j.talanta.2024.126790
- Athauda, T. J., Williams, W., Roberts, K. P., & Ozer, R. R. (2013). On the surface roughness and hydrophobicity of dual-size double-layer silica nanoparticles. *Journal of Materials Science*, *48*(18), 6115–6120. https://doi.org/10.1007/s10853-013-7407-5
- Ayesh, A. I., Thaker, S., Qamhieh, N., & Ghamlouche, H. (2011). Size-controlled Pd nanocluster grown by plasma gas-condensation method. *Journal of Nanoparticle Research*, *13*(3), 1125–1131. https://doi.org/10.1007/s11051-010-0104-2
- Baer, D. R., Engelhard, M. H., Johnson, G. E., Laskin, J., Lai, J., Mueller, K., Munusamy, P., Thevuthasan, S., Wang, H., Washton, N., Elder, A., Baisch, B. L., Karakoti, A., Kuchibhatla, S. V. N. T., & Moon, D. (2013). Surface characterization of nanomaterials and nanoparticles: Important needs and challenging opportunities. *Journal of Vacuum*

Science & Technology A: Vacuum, Surfaces, and Films, *31*(5), 050820. https://doi.org/10.1116/1.4818423

- Baer, D. R., Gaspar, D. J., Nachimuthu, P., Techane, S. D., & Castner, D. G. (2010). Application of surface chemical analysis tools for characterization of nanoparticles. *Analytical and Bioanalytical Chemistry*, *396*(3), 983–1002. https://doi.org/10.1007/s00216-009-3360-1
- Bapat, R. A., Chaubal, T. V., Joshi, C. P., Bapat, P. R., Choudhury, H., Pandey, M., Gorain, B., & Kesharwani, P. (2018). An overview of application of silver nanoparticles for biomaterials in dentistry. *Materials Science and Engineering: C*, *91*, 881–898. https://doi.org/10.1016/j.msec.2018.05.069
- Bellotti, R., Picotto, G. B., & Ribotta, L. (2022). AFM Measurements and Tip Characterization of Nanoparticles with Different Shapes. *Nanomanufacturing and Metrology*, *5*(2), 127–138. https://doi.org/10.1007/s41871-022-00125-x
- Beumer, K. (2012). A Matter of Scale: The Visual Representation of Nanotechnologies. *Spontaneous Generations: A Journal for the History and Philosophy of Science*, *6*(1), 65–74. https://doi.org/10.4245/sponge.v6i1.16139
- Beyene, H. D., Werkneh, A. A., Bezabh, H. K., & Ambaye, T. G. (2017). Synthesis paradigm and applications of silver nanoparticles (AgNPs), a review. *Sustainable Materials and Technologies*, *13*, 18–23. https://doi.org/10.1016/j.susmat.2017.08.001
- Bhushan, B. (Ed.). (2010). *Springer Handbook of Nanotechnology*. Springer Berlin Heidelberg. https://doi.org/10.1007/978-3-642-02525-9
- Burger, P., Singh, G., Johansson, C., Moya, C., Bruylants, G., Jakob, G., & Kalaboukhov, A. (2022). Atomic Force Manipulation of Single Magnetic Nanoparticles for Spin-Based Electronics. *ACS Nano*, *16*(11), 19253–19260. https://doi.org/10.1021/acsnano.2c08622
- Burlec, A. F., Corciova, A., Boev, M., Batir-Marin, D., Mircea, C., Cioanca, O., Danila, G., Danila, M., Bucur, A. F., & Hancianu, M. (2023). Current Overview of Metal Nanoparticles' Synthesis, Characterization, and Biomedical Applications, with a Focus on Silver and Gold Nanoparticles. *Pharmaceuticals*, *16*(10), 1410. https://doi.org/10.3390/ph16101410
- Buzea, C., Pacheco, I. I., & Robbie, K. (2007). Nanomaterials and nanoparticles: Sources and toxicity. *Biointerphases*, *2*(4), MR17–MR71. https://doi.org/10.1116/1.2815690
- Cappella, B., & Dietler, G. (1999). Force-distance curves by atomic force microscopy. *Surface Science Reports*, *34*(1–3), 1–104. https://doi.org/10.1016/S0167-5729(99)00003-5
- Chakraborty, I., & Pradeep, T. (2017). Atomically Precise Clusters of Noble Metals: Emerging Link between Atoms and Nanoparticles. *Chemical Reviews*, *117*(12), 8208–8271. https://doi.org/10.1021/acs.chemrev.6b00769
- Chen, D., Qiao, X., Qiu, X., & Chen, J. (2009). Synthesis and electrical properties of uniform silver nanoparticles for electronic applications. *Journal of Materials Science*, *44*(4), 1076–1081. https://doi.org/10.1007/s10853-008-3204-y

- Darwish, E., & Helmy, M. (2022). Effect of nanoparticles on surface roughness of digitally and conventionally constructed RPD framework. *Egyptian Dental Journal*, *68*(2), 1731–1739. https://doi.org/10.21608/edj.2022.123175.1993
- Duman, H., Eker, F., Akdaşçi, E., Witkowska, A. M., Bechelany, M., & Karav, S. (2024). Silver Nanoparticles: A Comprehensive Review of Synthesis Methods and Chemical and Physical Properties. *Nanomaterials*, *14*(18), 1527. https://doi.org/10.3390/nano14181527
- Eaton, P., & West, P. (2010). *Atomic Force Microscopy*.
- Elechiguerra, J. L., Burt, J. L., Morones, J. R., Camacho-Bragado, A., Gao, X., Lara, H. H., & Yacaman, M. J. (2005). Interaction of silver nanoparticles with HIV-1. *Journal of Nanobiotechnology*, *3*(1), 6. https://doi.org/10.1186/1477-3155-3-6
- El-Seedi, H. R., Omara, M. S., Omar, A. H., Elakshar, M. M., Shoukhba, Y. M., Duman, H., Karav, S., Rashwan, A. K., El-Seedi, A. H., Altaleb, H. A., Gao, H., Saeed, A., Jefri, O. A., Guo, Z., & Khalifa, S. A. M. (2024). Updated Review of Metal Nanoparticles Fabricated by Green Chemistry Using Natural Extracts: Biosynthesis, Mechanisms, and Applications. *Bioengineering*, *11*(11), 1095. https://doi.org/10.3390/bioengineering11111095
- Fahim, M., Shahzaib, A., Nishat, N., Jahan, A., Bhat, T. A., & Inam, A. (2024). Green synthesis of silver nanoparticles: A comprehensive review of methods, influencing factors, and applications. *JCIS Open*, *16*, 100125. https://doi.org/10.1016/j.jciso.2024.100125
- Fang, Q., & Lafdi, K. (2021). Effect of nanofiller morphology on the electrical conductivity of polymer nanocomposites. *Nano Express*, *2*(1), 010019. https://doi.org/10.1088/2632-959X/abe13f
- Farré, M., & Barceló, D. (2012). Introduction to the Analysis and Risk of Nanomaterials in Environmental and Food Samples. In *Comprehensive Analytical Chemistry* (Vol. 59, pp. 1–32). Elsevier. https://doi.org/10.1016/B978-0-444-56328-6.00001-3
- Firouz, F., Ebrahimi, J., Nikanjam, S., Farhadian, M., & Farmani, A. (2024). Effect of silver nanoparticles addition on the surface roughness of feldspathic porcelain. *Dental Cadmos*, *92*(03), 216. https://doi.org/10.19256/d.cadmos.03.2024.06
- Gadelmawla, E. S., Koura, M. M., Maksoud, T. M. A., Elewa, I. M., & Soliman, H. H. (2002). Roughness parameters. *Journal of Materials Processing Technology*, *123*(1), 133–145. https://doi.org/10.1016/S0924-0136(02)00060-2
- Giessibl, F. J. (2003). Advances in atomic force microscopy. *Reviews of Modern Physics*, *75*(3), 949–983. https://doi.org/10.1103/RevModPhys.75.949
- Gong, Y., Xu, J., & Buchanan, R. C. (2018). Surface roughness: A review of its measurement at micro-/nano-scale. *Physical Sciences Reviews*, *3*(1). https://doi.org/10.1515/psr-2017-0057
- Goodman, S. R. (Ed.). (2008). Tools of the Cell Biologist. In *Medical Cell Biology (Third Edition)* (Third Edition, pp. 1–26). Academic Press. https://doi.org/10.1016/B978-0-12-370458-0.50006-2

- Groot, P. J. De., & Lega, X. (2008). *Transparent film profiling and analysis by interference microscopy*. 70640I. https://doi.org/10.1117/12.794936
- Gulumian, M., Andraos, C., Afantitis, A., Puzyn, T., & Coville, N. J. (2021). Importance of Surface Topography in Both Biological Activity and Catalysis of Nanomaterials: Can Catalysis by Design Guide Safe by Design? *International Journal of Molecular Sciences*, *22*(15), 8347. https://doi.org/10.3390/ijms22158347
- Guo, D., Xie, G., & Luo, J. (2014). Mechanical properties of nanoparticles: Basics and applications. *Journal of Physics D: Applied Physics*, *47*(1), 013001. https://doi.org/10.1088/0022-3727/47/1/013001
- Güzel, R., & Erdal, G. (2018). Synthesis of Silver Nanoparticles. In K. Maaz (Ed.), *Silver Nanoparticles—Fabrication, Characterization and Applications*. InTech. https://doi.org/10.5772/intechopen.75363
- Habeeb Rahuman, H. B., Dhandapani, R., Narayanan, S., Palanivel, V., Paramasivam, R., Subbarayalu, R., Thangavelu, S., & Muthupandian, S. (2022). Medicinal plants mediated the green synthesis of silver nanoparticles and their biomedical applications. *IET Nanobiotechnology*, *16*(4), 115–144. https://doi.org/10.1049/nbt2.12078
- Herrero, Y. R., Camas, K. L., & Ullah, A. (2023). Characterization of biobased materials. In *Advanced Applications of Biobased Materials* (pp. 111–143). Elsevier. https://doi.org/10.1016/B978-0-323-91677-6.00005-2
- Ider, M., Abderrafi, K., Eddahbi, A., Ouaskit, S., & Kassiba, A. (2017). Silver Metallic Nanoparticles with Surface Plasmon Resonance: Synthesis and Characterizations. *Journal of Cluster Science*, *28*(3), 1051–1069. https://doi.org/10.1007/s10876-016-1080-1
- Iravani, S., Korbekandi, H., Mirmohammadi, S. V., & Zolfaghari, B. (2014). Synthesis of silver nanoparticles: Chemical, physical and biological methods. *Research in Pharmaceutical Sciences*, *9*(6), 385.
- Ishida, N. (2024). Atomic force microscopy. In *Non-Destructive Material Characterization Methods* (pp. 89–125). Elsevier. https://doi.org/10.1016/B978-0-323-91150-4.00011-2
- ISO 4287. (1997). *Specifications parameters*.
- ISO 25178. (2021). *Specifications Surface texture*.
- Israelachvili, J. N. (2011). *Intermolecular and Surface Forces*.
- Itakovi, N. (2019). PHYSICAL PROPERTIES OF NANOMATERIALS. *Vojnotehnicki Glasnik/Military Technical Courier*, *67*(1), 159–171.
- Jangid, H., Singh, S., Kashyap, P., Singh, A., & Kumar, G. (2024). Advancing biomedical applications: An in-depth analysis of silver nanoparticles in antimicrobial, anticancer, and wound healing roles. *Frontiers in Pharmacology*, *15*, 1438227. https://doi.org/10.3389/fphar.2024.1438227
- Jiang, K., Huang, Y., Zeng, G., Toma, F. M., Goddard, W. A., & Bell, A. T. (2020). Effects of Surface Roughness on the Electrochemical Reduction of CO_2 over Cu. *ACS Energy Letters*, *5*(4), 1206–1214. https://doi.org/10.1021/acsenergylett.0c00482

- Jouyban, A., & Rahimpour, E. (2020). Optical sensors based on silver nanoparticles for determination of pharmaceuticals: An overview of advances in the last decade. *Talanta, 217*, 121071. https://doi.org/10.1016/j.talanta.2020.121071
- Joy, D., & Ford, B. (2025, March 22). *Scanning electron microscope (SEM) | Definition, Images, Uses, Advantages, & Facts | Britannica*. https://www.britannica.com/technology/scanning-electron-microscope
- Khan, I., Abdalla, A., & Qurashi, A. (2017). Synthesis of hierarchical WO3 and Bi2O3/WO3 nanocomposite for solar-driven water splitting applications. *International Journal of Hydrogen Energy*, *42*(5), 3431–3439. https://doi.org/10.1016/j.ijhydene.2016.11.105
- Khan, I., Saeed, K., & Khan, I. (2019). Nanoparticles: Properties, applications and toxicities. *Arabian Journal of Chemistry*, *12*(7), 908–931. https://doi.org/10.1016/j.arabjc.2017.05.011
- Khatoon, U. T., Nageswara Rao, G. V. S., Mohan, K. M., Ramanaviciene, A., & Ramanavicius, A. (2017). Antibacterial and antifungal activity of silver nanospheres synthesized by tri-sodium citrate assisted chemical approach. *Vacuum*, *146*, 259–265. https://doi.org/10.1016/j.vacuum.2017.10.003
- Khayati, G. R., & Janghorban, K. (2012). The nanostructure evolution of Ag powder synthesized by high energy ball milling. *Advanced Powder Technology*, *23*(3), 393–397. https://doi.org/10.1016/j.apt.2011.05.005
- Kockert, M., Kojda, D., Mitdank, R., Mogilatenko, A., Wang, Z., Ruhhammer, J., Kroener, M., Woias, P., & Fischer, S. F. (2019). Nanometrology: Absolute Seebeck coefficient of individual silver nanowires. *Scientific Reports*, *9*(1), 20265. https://doi.org/10.1038/s41598-019-56602-9
- Kumar, S. (2021). *The coupled effect of surface roughness and nanoparticle size on the heat transfer enhancement of nanofluids for pool boiling*.
- Kyeyune, B. (2017). *Atomic Force Microscopy*. https://doi.org/10.13140/RG.2.2.17356.10887
- Lee, S. H., & Jun, B.-H. (2019). Silver Nanoparticles: Synthesis and Application for Nanomedicine. *International Journal of Molecular Sciences*, *20*(4), 865. https://doi.org/10.3390/ijms20040865
- Li, H., Gao, Y., Li, C., Ma, G., Shang, Y., & Sun, Y. (2016). A comparative study of the antibacterial mechanisms of silver ion and silver nanoparticles by Fourier transform infrared spectroscopy. *Vibrational Spectroscopy*, *85*, 112–121. https://doi.org/10.1016/j.vibspec.2016.04.007
- Li, Y., Liao, Q., Hou, W., & Qin, L. (2023). Silver-Based Surface Plasmon Sensors: Fabrication and Applications. *International Journal of Molecular Sciences*, *24*(4), Article 4. https://doi.org/10.3390/ijms24044142
- Li, Z., Dong, H., Wu, Z., Shen, J., Xu, D., He, R., Wan, L., & Zhang, S. (2020). Novel p-n type porous Ag2O/Bi5O7I heterojunction for Uv–Vis-NIR activated high efficient

photocatalytic degradation of bisphenol A: Photoelectric properties and degradation mechanism. *Applied Surface Science*, *529*, 147162. https://doi.org/10.1016/j.apsusc.2020.147162

- Liaqat, N., Jahan, N., Khalil-ur-Rahman, Anwar, T., & Qureshi, H. (2022). Green synthesized silver nanoparticles: Optimization, characterization, antimicrobial activity, and cytotoxicity study by hemolysis assay. *Frontiers in Chemistry*, *10*. https://doi.org/10.3389/fchem.2022.952006
- Lindsay, S. M. (2010). *Introduction to nanoscience*. Oxford University Press.
- Llorca, M., & Farré, M. (2023). Micromaterials and nanomaterials as potential emerging pollutants in the marine environment. In *Contaminants of Emerging Concern in the Marine Environment* (pp. 375–400). Elsevier. https://doi.org/10.1016/B978-0-323-90297-7.00005-6
- Lo, I. (2024). Semiconductor Nanomaterials for Optoelectronic Applications. *Nanomaterials*, *14*(23), Article 23. https://doi.org/10.3390/nano14231896
- Lyukshin, V., Shatko, D., & Strelnikov, P. (2021). Methods and approaches to the surface roughness assessment. *Materials Today: Proceedings*, *38*, 1441–1444. https://doi.org/10.1016/j.matpr.2020.08.122
- Mahadeshwara, M. (2022). *Stylus profilometer—About Tribology*. https://www.tribonet.org/wiki/stylus-profilometera-stylus-profilometer-is-a-contact-based-profilometer-that-brings-its-stylus-tip-into-direct-contact-with-the-measuring-surface-and-traces-the-desired-path-to-determine-the-topograp/
- Mahmudin, L., Suharyadi, E., Utomo, A. B. S., & Abraha, K. (2015). Optical Properties of Silver Nanoparticles for Surface Plasmon Resonance (SPR)-Based Biosensor Applications. *Journal of Modern Physics*, *06*(08), 1071–1076. https://doi.org/10.4236/jmp.2015.68111
- Marambio-Jones, C., & Hoek, E. M. V. (2010). A review of the antibacterial effects of silver nanomaterials and potential implications for human health and the environment. *Journal of Nanoparticle Research*, *12*(5), 1531–1551. https://doi.org/10.1007/s11051-010-9900-y
- Mekuye, B. (2024). The Impact of Size on the Optical Properties of Silver Nanoparticles Based on Dielectric Function. In S. Ameen, M. Shaheer Akhtar, A. Jiménez-Suárez, & G. Seisdedos (Eds.), *Nanotechnology and Nanomaterials Annual Volume 2024*. IntechOpen. https://doi.org/10.5772/intechopen.113976
- Mekuye, B., & Abera, B. (2023). Nanomaterials: An overview of synthesis, classification, characterization, and applications. *Nano Select*, *4*(8), 486–501. https://doi.org/10.1002/nano.202300038
- Menichetti, A., Mavridi-Printezi, A., Mordini, D., & Montalti, M. (2023). Effect of Size, Shape and Surface Functionalization on the Antibacterial Activity of Silver Nanoparticles. *Journal of Functional Biomaterials*, *14*(5), Article 5. https://doi.org/10.3390/jfb14050244
- Mohammed, A., & Abdullah, A. (2019). *Scanning Electron Microscopy (SEM): A Review*.

- Mohapatra, R. K. (2020). *Nanomaterials* (p. 16). Government College of Engineering Keonjhar.
- Mokobi, F. (2023, June 5). *Atomic Force Microscope: Principle, Parts, Uses - Microbe Notes*. https://microbenotes.com/atomic-force-microscope-afm/
- Montes Ruiz-Cabello, F. J., Fusco, S., Ibáñez-Ibáñez, P., Guerrero-Vacas, G., Cabrerizo-Vílchez, M. Á., & Rodríguez-Valverde, M. Á. (2023). Water-Repellent Galvanized Steel Surfaces Obtained by Sintering of Zinc Nanopowder. *Langmuir: The ACS Journal of Surfaces and Colloids*, *39*(15), 5469–5476. https://doi.org/10.1021/acs.langmuir.3c00182
- Mustapha, T., Misni, N., Ithnin, N. R., Daskum, A. M., & Unyah, N. Z. (2022). A Review on Plants and Microorganisms Mediated Synthesis of Silver Nanoparticles, Role of Plants Metabolites and Applications. *International Journal of Environmental Research and Public Health*, *19*(2), Article 2. https://doi.org/10.3390/ijerph19020674
- Myshkin, N. K., & Grigoriev, A. Y. (2013). *Roughness and Texture Concepts in Tribology*. *35*(2).
- Naumenko, K., Zahorodnia, S., Pop, C. V., & Rizun, N. (2023). Antiviral activity of silver nanoparticles against the influenza A virus. *Journal of Virus Eradication*, *9*(2), 100330. https://doi.org/10.1016/j.jve.2023.100330
- Nayak, M. K., Singh, J., Singh, B., Soni, S., Pandey, V. S., & Tyagi, S. (2017). Introduction to semiconductor nanomaterial and its optical and electronics properties. In *Metal Semiconductor Core-Shell Nanostructures for Energy and Environmental Applications* (pp. 1–33). Elsevier. https://doi.org/10.1016/B978-0-323-44922-9.00001-6
- Nayfeh, M. (Ed.). (2008). Chapter 7—Characterization and Simulation Technologies of Nanomaterial. In *Fundamentals and Applications of Nano Silicon in Plasmonics and Fullerines* (pp. 153–167). Elsevier. https://doi.org/10.1016/B978-0-323-48057-4.00007-4
- Nguyen, N. P. U., Dang, N. T., Doan, L., & Nguyen, T. T. H. (2023). Synthesis of Silver Nanoparticles: From Conventional to 'Modern' Methods—A Review. *Processes*, *11*(9), 2617. https://doi.org/10.3390/pr11092617
- Nie, P., Zhao, Y., & Xu, H. (2023). Synthesis, applications, toxicity and toxicity mechanisms of silver nanoparticles: A review. *Ecotoxicology and Environmental Safety*, *253*, 114636. https://doi.org/10.1016/j.ecoenv.2023.114636
- Nouailhat, A. (2006). *An Introduction to Nanoscience and Nanotechnology*.
- Olarte-Plata, J. D., Brekke-Svaland, G., & Bresme, F. (2020). The influence of surface roughness on the adhesive interactions and phase behavior of suspensions of calcite nanoparticles. *Nanoscale*, *12*(20), 11165–11173. https://doi.org/10.1039/D0NR00834F
- Oldenburg, S. (n.d.). *Silver Nanomaterials: Properties & Applications*. Retrieved April 20, 2025, from https://www.sigmaaldrich.com/IL/en/technical-documents/technical-article/materials-science-and-engineering/biosensors-and-imaging/silver-nanomaterials-properties?srsltid=AfmBOoq_nLHUqMcQxTyER0WqvKp2s0hOEGADMQYvkDZbTuQ112MOio8X

- Panja, A. (2021). Silver Nanoparticles – A Review. *Eurasian Journal of Medicine and Oncology*. https://doi.org/10.14744/ejmo.2021.59602
- Putman, C., Van Der Werf, K. O., De Grooth, B. G., Van Hulst, N. F., & Greve, J. (1994). Tapping mode atomic force microscopy in liquid. *Applied Physics Letters*, *64*(18), 2454–2456. https://doi.org/10.1063/1.111597
- Ramesh, M., Anbuvannan, M., & Viruthagiri, G. (2015). Green synthesis of ZnO nanoparticles using Solanum nigrum leaf extract and their antibacterial activity. *Spectrochimica Acta Part A: Molecular and Biomolecular Spectroscopy*, *136*, 864–870. https://doi.org/10.1016/j.saa.2014.09.105
- Rana, M. S., Pota, H. R., & Petersen, I. R. (2017). Improvement in the Imaging Performance of Atomic Force Microscopy: A Survey. *IEEE Transactions on Automation Science and Engineering*, *14*(2), 1265–1285. https://doi.org/10.1109/TASE.2016.2538319
- Ravi, N., Markandeya, R., & Joshi, S. V. (2017). Effect of substrate roughness on adhesion and tribological properties of nc-TiAlN/a-Si_3 N_4 nanocomposite coatings deposited by cathodic arc PVD process. *Surface Engineering*, *33*(1), 7–19. https://doi.org/10.1179/1743294415Y.0000000005
- Roco, M. C. (2003). Nanotechnology: Convergence with modern biology and medicine. *Current Opinion in Biotechnology*, *14*(3), 337–346. https://doi.org/10.1016/s0958-1669(03)00068-5
- Ruzova, T. A., & Haddadi, B. (2025). Surface roughness and its measurement methods—Analytical review. *Results in Surfaces and Interfaces*, *19*, 100441. https://doi.org/10.1016/j.rsurfi.2025.100441
- Saadat, S., Pandey, G., Tharmavaram, M., Braganza, V., & Rawtani, D. (2020). Nano-interfacial decoration of Halloysite Nanotubes for the development of antimicrobial nanocomposites. *Advances in Colloid and Interface Science*, *275*, 102063. https://doi.org/10.1016/j.cis.2019.102063
- Sahu, M. K. (2019). *Semiconductor Nanoparticles Theory and Applications*. *14*(2).
- Saleh, T. A. (2022). Properties of nanoadsorbents and adsorption mechanisms. In *Interface Science and Technology* (Vol. 34, pp. 233–263). Elsevier. https://doi.org/10.1016/B978-0-12-849876-7.00010-5
- Sayab, A. (2024). *Semiconductor Nanoparticles: Synthesis, Characterization, and Theoritical Analysis of Electronic and Structural Properties* [Master Thesis]. University of Kerbala.
- Sedin, D. L., & Rowlen, K. L. (2001). Influence of tip size on AFM roughness measurements. *Applied Surface Science*, *182*(1–2), 40–48. https://doi.org/10.1016/S0169-4332(01)00432-9
- Serna-Gallén, P., & Mužina, K. (2024). Metallic nanoparticles at the forefront of research: Novel trends in catalysis and plasmonics. *Nano Materials Science*, S2589965124001570. https://doi.org/10.1016/j.nanoms.2024.10.009

- Shahalaei, M., Azad, A. K., Sulaiman, W. M. A. W., Derakhshani, A., Mofakham, E. B., Mallandrich, M., Kumarasamy, V., & Subramaniyan, V. (2024). A review of metallic nanoparticles: Present issues and prospects focused on the preparation methods, characterization techniques, and their theranostic applications. *Frontiers in Chemistry*, *12*. https://doi.org/10.3389/fchem.2024.1398979
- Siddiqi, K. S., Husen, A., & Rao, R. A. K. (2018). A review on biosynthesis of silver nanoparticles and their biocidal properties. *Journal of Nanobiotechnology*, *16*(1), 14. https://doi.org/10.1186/s12951-018-0334-5
- Siegel, R. W. (1992). *NANOSTRUCTURED MATERIALS*.
- Singh, J., Dutta, T., Kim, K.-H., Rawat, M., Samddar, P., & Kumar, P. (2018). 'Green' synthesis of metals and their oxide nanoparticles: Applications for environmental remediation. *Journal of Nanobiotechnology*, *16*(1), 84. https://doi.org/10.1186/s12951-018-0408-4
- Singh, V., Yadav, S. S., Chauhan, V., Shukla, S., & Vishnolia, K. K. (2021). Applications of Nanoparticles in Various Fields: In D. Yadav, A. Bansal, M. Bhatia, M. Hooda, & J. Morato (Eds.), *Advances in Medical Technologies and Clinical Practice* (pp. 221–236). IGI Global. https://doi.org/10.4018/978-1-7998-6527-8.ch011
- Sportelli, M. C., Izzi, M., Volpe, A., Clemente, M., Picca, R. A., Ancona, A., Lugarà, P. M., Palazzo, G., & Cioffi, N. (2018). The Pros and Cons of the Use of Laser Ablation Synthesis for the Production of Silver Nano-Antimicrobials. *Antibiotics*, *7*(3), 67. https://doi.org/10.3390/antibiotics7030067
- Sreelatha, K., AnandaKumar, C. S., Saraswathi, M., Anusha, P., Rose, N. M., & Bhargava, D. (2025). A Comprehensive Review of Nanoparticle Characterization Techniques. *International Journal of Research and Review*, *12*(1), 194–200. https://doi.org/10.52403/ijrr.20250124
- Stagon, S. P., & Huang, H. (2013). Syntheses and applications of small metallic nanorods from solution and physical vapor deposition. *Nanotechnology Reviews*, *2*(3), 259–267. https://doi.org/10.1515/ntrev-2013-0001
- Sugimoto, Y., Pou, P., Abe, M., Jelinek, P., Pérez, R., Morita, S., & Custance, Ó. (2007). Chemical identification of individual surface atoms by atomic force microscopy. *Nature*, *446*(7131), 64–67. https://doi.org/10.1038/nature05530
- T. Galatage, S., S. Hebalkar, A., V. Dhobale, S., R. Mali, O., S. Kumbhar, P., V. Nikade, S., & G. Killedar, S. (2021). Silver Nanoparticles: Properties, Synthesis, Characterization, Applications and Future Trends. In S. Kumar, P. Kumar, & C. Shakher Pathak (Eds.), *Silver Micro-Nanoparticles—Properties, Synthesis, Characterization, and Applications*. IntechOpen. https://doi.org/10.5772/intechopen.99173
- Temiz, C. (2022). Scanning Electron Microscopy. In M. Mhadhbi (Ed.), *Electron Microscopy*. IntechOpen. https://doi.org/10.5772/intechopen.103956

- Tien, D. C., Liao, C. Y., Huang, J. C., Tseng, K. H., Lung, J. K., Tsung, T. T., Kao, W. S., Tsai, T. H., Cheng, T. W., & Yu, B. S. (2008). Novel technique for preparing a nano-silver water suspension by the arc-discharge method. *Rev. Adv. Mater. Sci*, *18*(8), 752–758.
- Tighe, T., & Kiemle, S. (2011). *Atomic Force Microscopy*. Materials Research Institute. https://www.mri.psu.edu/materials-characterization-lab/characterization-techniques/atomic-force-microscopy?utm_source=chatgpt.com
- Treebupachatsakul, T., Shinnakerdchoke, S., & Pechprasarn, S. (2021). Analysis of Effects of Surface Roughness on Sensing Performance of Surface Plasmon Resonance Detection for Refractive Index Sensing Application. *Sensors*, *21*(18), 6164. https://doi.org/10.3390/s21186164
- Triampo, D., & Triampo, W. (2009). The Working of the Atomic Force Microscope for Chemical Mapping. *The Open Materials Science Journal*, *3*(1), 50–55. https://doi.org/10.2174/1874088X00903010050
- Tripathy, S. (2023). Top-down and Bottom-up Approaches for Synthesis of Nanoparticles. In J. N. Cruz (Ed.), *Materials Research Foundations* (1st ed., Vol. 145, pp. 92–130). Materials Research Forum LLC. https://doi.org/10.21741/9781644902370-4
- Ul-Islam, M., Ullah, M. W., Khan, T., & Park, J. K. (2021). Bacterial cellulose: Trends in synthesis, characterization, and applications. In *Handbook of Hydrocolloids* (pp. 923–974). Elsevier. https://doi.org/10.1016/B978-0-12-820104-6.00010-3
- Ullah Khan, M., Ullah, H., Honey, S., Talib, Z., Abbas, M., Umar, A., Ahmad, T., Sohail, J., Sohail, A., Makgopa, K., Ahmad, J., & Asim, J. (2023). Metal Nanoparticles: Synthesis Approach, Types and Applications – A Mini Review. *Nano-Horizons*, *2*. https://doi.org/10.25159/NanoHorizons.87a973477e35
- Upadhyay, K., Tamrakar, R. K., Thomas, S., & Kumar, M. (2023). Surface functionalized nanoparticles: A boon to biomedical science. *Chemico-Biological Interactions*, *380*, 110537. https://doi.org/10.1016/j.cbi.2023.110537
- Vaculikova, E., Cernikova, A., Placha, D., Pisarcik, M., Peikertova, P., Dedkova, K., Devinsky, F., & Jampilek, J. (2016). Preparation of Hydrochlorothiazide Nanoparticles for Solubility Enhancement. *Molecules*, *21*(8), 1005. https://doi.org/10.3390/molecules21081005
- Vahabi, S., Nazemi Salman, B., & Javanmard, A. (2013). Atomic force microscopy application in biological research: A review study. *Iranian Journal of Medical Sciences*, *38*(2), 76–83.
- Vanlalveni, C., Lallianrawna, S., Biswas, A., Selvaraj, M., Changmai, B., & Rokhum, S. L. (2021). Green synthesis of silver nanoparticles using plant extracts and their antimicrobial activities: A review of recent literature. *RSC Advances*, *11*(5), 2804–2837. https://doi.org/10.1039/d0ra09941d
- Varga, M., Prokeˇs, J., Bober, P., & Stejskal, J. (2012). *Electrical Conductivity of Polyaniline–Silver Nanocomposites*. 52–57.

- Veerapandian, M., & Yun, K. (2009). Study of Atomic Force Microscopy in Pharmaceutical and Biopharmaceutical Interactions—A Mini Review. *Current Pharmaceutical Analysis*, *5*(3), 256–268. https://doi.org/10.2174/157341209788922020
- Veerasamy, R., Xin, T. Z., Gunasagaran, S., Xiang, T. F. W., Yang, E. F. C., Jeyakumar, N., & Dhanaraj, S. A. (2011). Biosynthesis of silver nanoparticles using mangosteen leaf extract and evaluation of their antimicrobial activities. *Journal of Saudi Chemical Society*, *15*(2), 113–120. https://doi.org/10.1016/j.jscs.2010.06.004
- Weng, L., Zhang, L., Chen, Y. P., & Rokhinson, L. P. (2008). Atomic force microscope local oxidation nanolithography of graphene. *Applied Physics Letters*, *93*(9), 093107. https://doi.org/10.1063/1.2976429
- Wilson, R. A., & Bullen, H. A. (2006). *Atomic Force Microscopy*.
- Wyant, J. (2016). *White Light Interferometry*. *4737*.
- Xu, K., & Leng, H. (2024). Quantitative wear evaluation of tips based on sharp structures. *Beilstein Journal of Nanotechnology*, *15*, 230–241. https://doi.org/10.3762/bjnano.15.22
- Xue, J., Zhu, Y., Bai, S., He, C., Du, G., Zhang, Y., Zhong, Y., Chen, W., Wang, H., & Sun, X. (2022). Nanoparticles with rough surface improve the therapeutic effect of photothermal immunotherapy against melanoma. *Acta Pharmaceutica Sinica B*, *12*(6), 2934–2949. https://doi.org/10.1016/j.apsb.2021.11.020
- Yaqoob, A. A., Umar, K., & Ibrahim, M. N. M. (2020). Silver nanoparticles: Various methods of synthesis, size affecting factors and their potential applications–a review. *Applied Nanoscience*, *10*(5), 1369–1378. https://doi.org/10.1007/s13204-020-01318-w
- Yousaf, S., & Ali, S. (2007). *INTRODUCTION TO NANOSCIENCE*. 11–20.
- Żarowska, B., Koźlecki, T., Piegza, M., Jaros-Koźlecka, K., & Robak, M. (2019). New Look on Antifungal Activity of Silver Nanoparticles (AgNPs). *Polish Journal of Microbiology*, *68*(4), 515–525. https://doi.org/10.33073/pjm-2019-051
- Zhang, X.-F., Liu, Z.-G., Shen, W., & Gurunathan, S. (2016). Silver Nanoparticles: Synthesis, Characterization, Properties, Applications, and Therapeutic Approaches. *International Journal of Molecular Sciences*, *17*(9), 1534. https://doi.org/10.3390/ijms17091534
- Zhou, P., Yu, H., Yang, W., Wen, Y., Wang, Z., Li, W. J., & Liu, L. (2017). Spatial Manipulation and Assembly of Nanoparticles by Atomic Force Microscopy Tip-Induced Dielectrophoresis. *ACS Applied Materials & Interfaces*, *9*(19), 16715–16724. https://doi.org/10.1021/acsami.7b03565

تحليل خشونة سطح جسيمات الفضة النانوية باستخدام مجهر القوة الذرية

اعداد: رنيم منصور عبد القادر محمد

اشراف:

مشرف أول: د. حسين السمامرة

مشرف ثان: د. اسحق موسى

ملخص

هدفت هذه الدراسة إلى تحليل تأثير مجموعة من العوامل الفيزيائية على خشونة سطح جسيمات الفضة النانوية، باستخدام مجهر القوة الذرية كأداة تحليلية رئيسية، إلى جانب برنامج حاسوبي.

ركز البحث على أربعة متغيرات لفهم تأثيرها على خشونة السطح: حجم جسيمات الفضة النانوية، وتركيز الجسيمات أثناء عملية التصنيع، ونوع رأس المجس المستخدم (حاد، قياسي)، وطريقة تصنيع الجسيمات (الطريقة الفيزيائية والطريقة الخضراء).

أظهرت النتائج وجود علاقة مباشرة بين حجم الجسيمات وخشونة السطح، فكلما زاد حجم الجسيمات، ارتفعت قيم خشونة السطح، مما يعكس تأثير الجسيمات الأكبر على بنية السطح بشكل كبير عند بناء المواد النانوية.

في المقابل، لوحظت علاقة عكسية بين تركيز جسيمات الفضة النانوية أثناء عملية التصنيع وخشونة السطح، حيث انخفضت قيم الخشونة بشكل ملحوظ مع زيادة تركيز الجسيمات، وتم تفسير ذلك بأن وجود عدد أكبر من الجسيمات يساعد في تغطية أكثر اتساقًا لسطح العينة.

كما وُجد أن استخدام طرف حاد أدى إلى الحصول على قيم خشونة سطح أعلى مقارنةً بالطرف القياسي، وذلك بسبب زيادة حساسية الطرف الحاد لبنية سطح العينة، مما أدى إلى قياسات أكثر دقة.

وأخيرًا، كشفت المقارنة بين طريقتي التصنيع الفيزيائي والخضراء لتحضير جسيمات النانو الفضية عن تباين واضح في قيم الخشونة، فقد وقعت قيم الخشونة التي تم الحصول عليها من الطريقة الفيزيائية بين القيم التي تم الحصول عليها من تركيزين مختلفين (30 و70 ملغ/ مل) في طريقة التصنيع الأخضر، وكانت أقرب إلى التركيز الأعلى (70 ملغ/ مل)، مما يشير إلى تأثر خشونة سطح الجسيمات النانوية بطرق التخليق المختلفة.

وتدعم هذه النتائج أهمية ضبط ظروف تخليق وتحليل الجسيمات النانوية لاستخدامها بفعالية في تطبيقات النانو، نظرًا لتأثيرها المباشر على خصائص السطح، والتي تلعب دورًا حاسمًا في أداء المواد في مختلف مجالات التطبيق مثل الطب والاستشعار والتحفيز.